

Measurement Systems for Estimating Imposed Loads

- A Study on a Cross Laminated Timber Slab



Mätsystem för att uppskatta nyttiga laster
- En studie på ett bjälklag av korslimmat trä

Cassandra Doggett 2022

Division of Structural Engineering
Faculty of Engineering, LTH
P.O. Box 118
S-221 00 LUND
Sweden

Avdelningen för Konstruktionsteknik
Lunds Tekniska Högskola
Box 118
221 00 LUND

Rapport TVBK-5292
ISSN: 0349-4969
ISRN: LUTVDG/TVBK-22/5292

Master's Thesis
Supervisors: Ivar Björnsson och Oskar Larsson Ivanov
June, 2022

Abstract

The construction sector stands for eleven percent of the carbon dioxide emissions in the world WorldGBC (2019). To minimize that impact, the construction sector must take a closer look at improving the sustainability of buildings. One way to do this would be to have a more accurate understanding of the loads that affect buildings, including the so-called imposed load. The imposed load includes loads that arise due to the normal occupancy of humans and furniture. This load is of particular interest due to timber having a relatively low self-weight in relation to the imposed loads.

The aim of this study is to investigate how accurately different measurement systems can measure imposed loads in buildings. Today imposed loads are based on outdated research with limited grounds. There are not enough studies conducted to be able to determine an accurate design load. To find a more accurate design load the accuracy of the measurement systems was tested in a few different situations. The tests were limited to strain gauges and potentiometers and were conducted on a cross laminated timber (CLT) slab which was then subjected to different loads. By comparing the real loads to the calculated loads from the measurements, it was possible to find the uncertainty associated with these measurements. By implementing measurement systems in real load situations, a broader database of real loads could be collected. This could in turn lead to finding an improved value for the imposed loads.

The study concluded that it was possible to measure the load on a CLT slab with the help of strain gauges and potentiometers. The best overall accuracy had an error of eight percent for a centrally placed strain gauge and the average error was about twenty percent. It could therefore be concluded that measurement systems could be a solution to finding a more accurate imposed load, which would allow for more precise dimensions and more efficient material usage. This may in turn have a great impact on improving sustainability within the building sector.

Keywords: strain gauge, potentiometer, measurement system, sensor, cross laminated timber, imposed load, live load, design standard, sustainability, CLT

Sammanfattning

Byggbranschen står för elva procent av koldioxidutsläppen i världen (WorldGBC, 2019). För att minimera den påverkan måste byggbranschen förbättra byggnaders hållbarhet. Detta skulle kunna göras genom att få en mer exakt förståelse för de laster som påverkar byggnader. En av de laster som påverkar dimensioneringen av byggnader är den nyttiga lasten. Den nyttiga lasten beror på belastningar som uppstår på grund av människors vanliga bruk av byggnader. När det gäller nyttiga laster bör särskild fokus läggas på träkonstruktioner. Detta på grund av att trä har en relativt låg egenvikt och påverkas därför i en större utsträckning av de nyttiga lasterna.

Syftet med detta examensarbete är att undersöka och konstatera mätprecisionen för olika mätsystem. Om en tillräckligt bra precision uppnås kan det finnas möjlighet att utnyttja mätsystem för att hitta ett mer verkligt värde för de nyttiga lasterna. Detta skulle uppnås genom att använda mätsystemen för att samla in data från verkliga situationer. De dimensionerande värdena för nyttiga laster består idag av utdaterad forskning med en begränsad grund. Det finns inte tillräckligt många studier utförda för att kunna fastställa en exakt dimensionerande last, särskilt för en last som har så pass stor inflytande på dimensioneringen. För att hitta en mer exakt dimensionerande last testades mätsystemens noggrannhet i några olika situationer. Testerna var begränsade till töjningsgivare och potentiometer och utfördes på ett bjälklag av korslimmat trä (KL-trä) som sedan utsattes för olika belastningar. Genom att jämföra de verkliga lasterna med de beräknade laster från mätningarna, var det möjligt att konstatera noggrannheten hos dessa mätningar.

Examensarbetets slutsats visade att det var möjligt att mäta belastningen på ett KL-träbjälklag med hjälp av töjningsgivare och potentiometrar. Den mest noggranna mätningen hade en felmarginal på åtta procent för ett centralt placerat mätsystem och medelvärdet för felmarginalen var cirka tjugo procent. Sådan precision har potential till att ytterligare precisera värdet för den nyttiga lasten, vilket skulle möjliggöra mer exakta dimensioner och effektivare materialanvändning. Detta kan i sin tur ha en positiv påverkan på byggsektorns framtida hållbarhet.

Nyckelord: töjningsgivare, potentiometer, mätsystem, sensor, korslimmat trä, nyttig last, dimensioneringsnorm, hållbarhet, KLT

Acknowledgements

This master's thesis was conducted during spring 2022 at the Division of Structural Engineering at Lund's Faculty of Engineering, LTH. The master's thesis was written as a conclusion of my five-year civil engineering degree, specializing in construction.

I would like to express my gratitude for all the help and guidance I have received while writing my thesis. First and foremost, to my supervisors, Ivar Björnsson at the Division of Structural Engineering who with his expertise gave me a large perspective on my thesis topic and to Oscar Larsson Ivanov from Boverket who shared his knowledge and experiences and came up with the original idea for this thesis. Secondly, I would like to thank John Leander for his expert advice on sensors and lab technician Stefan Backe whose expert knowledge in the lab allowed me to conduct my experiments. Finally, I would like to thank the Tyréns office in Malmö for giving me the opportunity to visit their office while writing my thesis, they have given me great inspiration in the field of construction and been a great support while writing my thesis.

I would also like to thank my family for their unwavering support during my years of study and direct a heartfelt thanks to all the friends I have made during my time at Lund University.

Lund, June 2022

Cassandra Doggett

Notations and Symbols

$E_{m,90,\text{mean}}$ - modulus of elasticity perpendicular to the grain

$E_{m,0,\text{mean}}$ - modulus of elasticity parallel to the grain

E – modulus of elasticity

f_{mk} – bending strength parallel to the fibers

f_{md} – design bending strength parallel to the fibers

$G_{90,2}$ – mean value of the modulus of rolling shear

h - height

I – moment of inertia

$I_{y,\text{net}}$ – net moment of inertia

I_{ef} – effective moment of inertia

L – length

L_{ref} – reference length

EI – bending stiffness

P – point load

q_k – uniformly distributed load

Q_k – point load

v – deformation

w - width

γ – gamma

ε – strain

σ – stress

Table of Contents

1	Introduction.....	1
1.1	Background	1
1.2	Purpose and thesis questions	2
1.3	Limitations	2
1.4	Outline.....	3
2	Theory.....	4
2.1	Definition of load types.....	4
2.1.1	Imposed load.....	5
2.1.2	Dynamic loads	9
2.2	Timber structures.....	9
2.2.1	Timber grading.....	10
	Modulus of Elasticity	11
2.2.2	Cross laminated timber (CLT).....	11
2.2.3	Sustainability.....	13
2.3	Structural health monitoring.....	13
2.3.1	Bridge Weigh in Motion (BWIM).....	14
2.4	Measurement systems	15
2.4.1	Measurands	16
2.4.2	Types of measurement systems	16
2.4.3	Placement of the measurement systems.....	20
3	Method.....	22
3.1	Material	22
3.1.1	CLT slab.....	22
3.1.2	Placement of the measurement systems in this study	23
3.2	Analytical method	25
3.2.1	Load cases.....	25
3.2.2	Deformation calculations	26
3.2.3	Strain calculations.....	26
3.2.4	Moment of inertia	27
3.2.5	Bending stiffness.....	29
3.3	Execution of the tests	29
3.3.1	Test 1: Hydraulic actuator.....	29

3.3.2	Test 2: Beam dead-loads	30
3.3.3	Test 3: Load from people	32
3.3.4	Test 4: Unknown load	33
3.3.5	Test 5: Test to failure	33
4	Results and discussion	34
4.1	Test 1: Hydraulic actuator	34
4.2	Test 2: Dead-weight loading	35
4.3	Test 3: Load from people	37
4.4	Test 4: Unknown load	37
4.4.1	Real load situation revealed	40
4.5	Test 5: Test to failure	40
5	Calculations.....	43
5.1	Test 1: Hydraulic actuator	43
5.2	Test 2: Dead-weight loading	45
5.3	Test 3: Load from people	48
5.4	Test 4: Unknown load	49
5.4.1	Real load situation revealed	51
6	Discussion	52
7	Conclusion	55
8	Future studies	56
9	References.....	57
	Appendix A.....	62
	Appendix B	63
	Appendix C.....	65
	Appendix D.....	66
	Appendix E	68
	Appendix F.....	69

1 Introduction

1.1 Background

When thinking of the future, sustainability and being environmentally conscious are growing trends. The material used and the construction of buildings is responsible for 11 percent of all carbon dioxide emissions in the world (WorldGBC, 2019). This must change. Using wood as a structural material may be a part of the solution. Timber is one of the building materials that requires the least energy during its life cycle and has lower carbon dioxide emissions than many other commonly used building materials (Shmulsky and Jones, 2019). An increased use of timber in building construction may provide a potentially significant reduction to the negative environmental impacts generated by the construction sector. In order to reach this reduction, more information is needed on how to properly design timber buildings and how to consider the impact of loads on these buildings.

One of the loads that impact buildings is imposed loads. These loads occur due to furniture, equipment, and the normal occupancy of people in buildings. There is limited information on how the given values for imposed loads in the structural Eurocodes have been determined. A few different publications have dealt with the subject, including Sentler (1974), Honfi (2014) and Bengtsson and Sandberg (2020). These papers have all concluded that there is a lack of information regarding imposed loads and that more information is required. Loads directly impact the amount of material used. By finding more exact loads dimensions can become more precise and possibly lead to more optimized material use.

One method that can be used to determine a more suitable representation of the imposed loads is through advanced measurement systems. Measurement systems are an advancing technology and there are many different types. In the building sector, measurement systems are primarily used to measure deformation and strain which can be used to calculate other values such as the load and stress. With the help of measurement systems, it may be possible to better understand imposed loads by measuring the deformation that has occurred. With the measured deformation the loads that the beam or slab are exposed to can then be calculated. Using this method measurement systems can be used to work proactively towards preventing unexpected loads from destroying a building. For example, the measurement systems could be set to a maximum deformation, if this level were reached it would be understood that the structure needed to be reinforced. By reinforcing the structure a potential collapse could be prevented. In a worst-case scenario the structure could be dismantled before a collapse where possible injuries could occur to people or damage to other nearby structures.

This study will focus on timber, as a building material. Timber is relatively lightweight in comparison to concrete. The lightweight timber can be seen as an advantage due to a smaller load but this also comes with its disadvantages. The most important disadvantage for this project is that the imposed load has a much greater impact on the dimensions needed for timber due to the lower self-load. Another aspect to consider is the fact that the structural safety is directly impacted by the ratio between the live and dead load. Due to a greater amount of

uncertainty for the live load, a higher relative level of this load leads to a higher relative level of uncertainty and subsequently lower levels of safety.

1.2 Purpose and thesis questions

The purpose of this study is to investigate the different types of measurement systems that are appropriate for providing a more representative basis for determining new design imposed loads in the structural codes. Firstly, a literature study will be presented, discussing previous research on this topic. Secondly a test will be executed where a cross laminated timber (CLT) slab will be subjected to different load situations. By measuring the slab's response, the load that the slab was subjected to can be estimated. The aim is to be able to draw conclusions on the measurement systems future potential for acquiring more data on imposed loads, by assessing the accuracy of these calculated loads. The acquired data then has the potential to be used to update the values provided in the design code.

The thesis questions are presented below.

- **How accurately can the load affecting a CLT slab, in a building, be calculated by using measurement data from measurement systems?**
- **How feasible is it to use different measurement systems for imposed loads?**
- **How could a measurement system be designed in a realistic situation?**

1.3 Limitations

In this study the focus is on loads in offices and residential buildings. Different load types will be described, one type of load is dynamic loads which can result in vibrations which is particularly important for light floor structures such as CLT. Vibrations will not be further mentioned but are an important aspect when considering imposed loads on timber slabs. Time dependent loads are the predominant load type that affect floors in actual buildings but due to time limitations in this study the loads will be short term.

Different types of timber slabs will be described but composite floor structures, such as timber and concrete, will not be discussed.

A brief description of different sensors will be covered, but no deeper investigation into the technical functioning of the sensors will be given.

In order to simplify the calculations, the load on the slab in test 1 was considered as a point load on a simply supported beam instead of a linear load in the middle of the slab. These load situations are rather similar so potential errors should not be too great. This resulted in a two-dimensional problem instead of a three-dimensional problem and therefore a load case could be used. The tests were also simplified by only focusing on short term loads.

1.4 Outline

A literature review will be presented in chapter 2. This chapter will cover a brief description of timber as a building material, the use of timber slabs in buildings, the historical background of imposed loads and a description of different load types. In chapter 3 the method for the study is described, both the method used for the execution of the experiment and the calculations required. Chapter 4 will present the results from the study and a brief discussion of the results. In chapter 5 the results from the calculations will be presented and a further discussion of the results will be conducted. In chapter 6 a more in-depth discussion of the results will be conducted and finally in chapter 7 conclusions will be drawn.

2 Theory

The aim of this chapter is to give an understanding of the different theoretical aspects underlying this study. Firstly, different load types will be described, in particular different aspects that impact loads such as time and space. Secondly timber structures will be described to gain understanding as to how the CLT slab will react in the test. Thirdly structural health monitoring will be briefly introduced, and finally different measurement systems and terms related to measurement systems will be presented.

2.1 Definition of load types

The dimensions of the load bearing structures (i.e. buildings) are determined by considering the loads acting upon it. In this thesis only the CLT slab will be investigated and the potential loads on it. In reality there are loads from other structures such as the walls and the roof. Loads can be divided into categories based on their origin such as loads from self-weight, wind, snow and imposed loads. Another categorization method that is used is based on loads variation in time and space. When considering the variation over time, there are two types: permanent and variable. The focus in this study will be on the variable action which can be divided into static, dynamic, fatigue and long-term loads. The different categories are based on how long the loads last. When considering loads in offices and residential buildings the most relevant category is therefore the long-term loads which have a duration of six months to 10 years, or permanent loads which last more than 10 years (SIS, 1991). The variation in space can be divided into fixed or free loads. These different types of loads are depicted in figure 2.1.

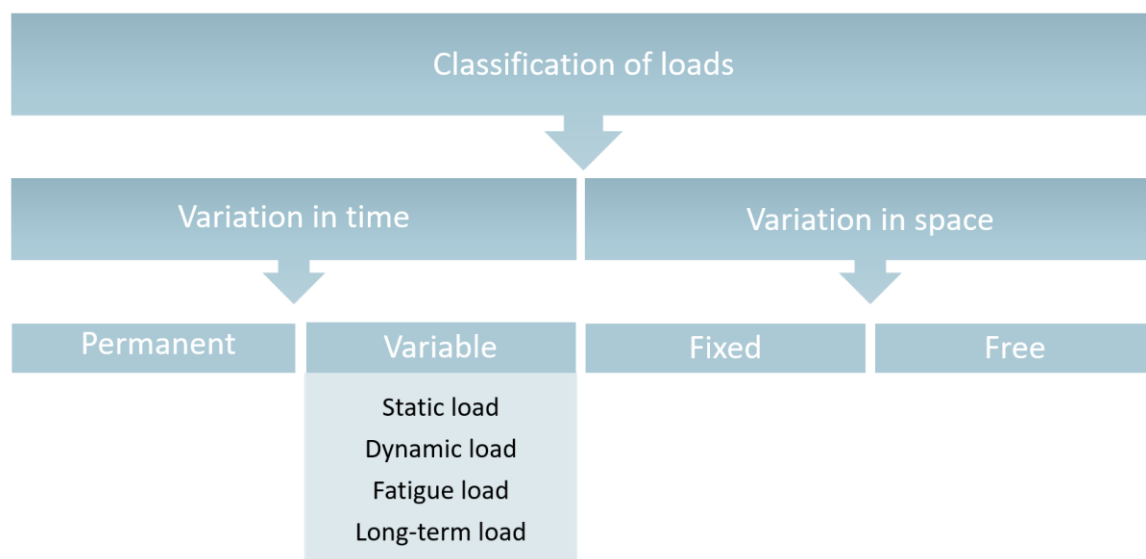


Figure 2.1: Classification of loads after Isaksson et al. (2011)

In structural design, design loads are used to ensure a satisfactory level of safety against collapse for the structure designed. The target degrees of safety are prescribed in the design codes which are used to calibrate the partial safety factors in the code for both loads and resistance factors. However, a design imposed load that is too high leads to buildings being

built using excess material while using a load that is too low may lead to buildings that are unsafe. Design loads are calculated from the characteristic load with applied partial safety factors. The characteristic load is defined as the 98 percentile for the static distribution for the yearly maximum according to figure 2.2 (Isaksson et al., 2011).

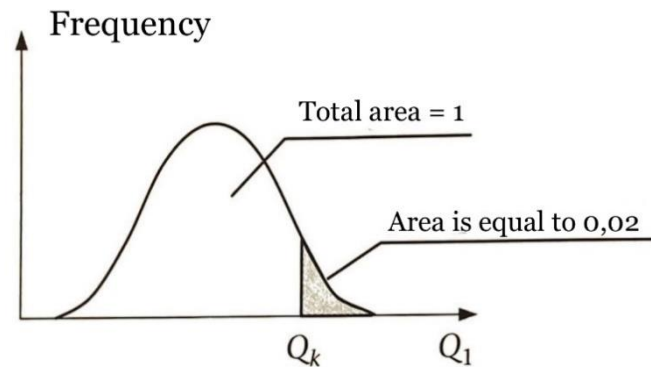


Figure 2.2: Definition of the characteristic value for the variable load where Q_1 represents the yearly maximum for the load and Q_k represents the characteristic load. The figure was used with permission from Isaksson et al. (2011)

When designing structures in structural engineering a method called limit state design can be used where the limit state is the state at which a structure is at the limit of not fulfilling the requirements it is designed for. There are two limits that are predominantly used, the ultimate limit state and the serviceability limit state. The ultimate limit state refers to the complete structural failure and the serviceability limit state refers to the functional use of the structure, but collapse is not expected (Isaksson et al., 2011).

2.1.1 Imposed load

Imposed loads, also known as live loads, are classified according to Eurocode as “variable free actions” (SIS, 1991). This entails that the loads vary both over time and in space. This study aims to measure loads that represent potential imposed loads in real situations. The aspect of measuring both time and space would create very complicated calculations, therefore a few simplifications were made as mentioned previously.

2.1.1.1 Categorization based on time variation

The International Council for Research and Innovation in Building and Construction (CIB) divide imposed loads into two categories: *sustained* and *intermittent loads*. The sustained loads can be further divided into two categories (CIB, 1989). The first category includes loads from furniture which generally vary very little over time apart from special situations when moving or reorganizing furniture, this is depicted in figure 2.3a. The other category consists of the loads created by occupancy and normal use by people. This is depicted in figure 2.3b. Finally figure 2.3c depicts situations where the load is significantly increased over short amounts of time. This is the intermittent load which includes loads from rare events. These events are unpredictable and can be due to concentrations of people, for example parties or from moving objects and reorganizing.

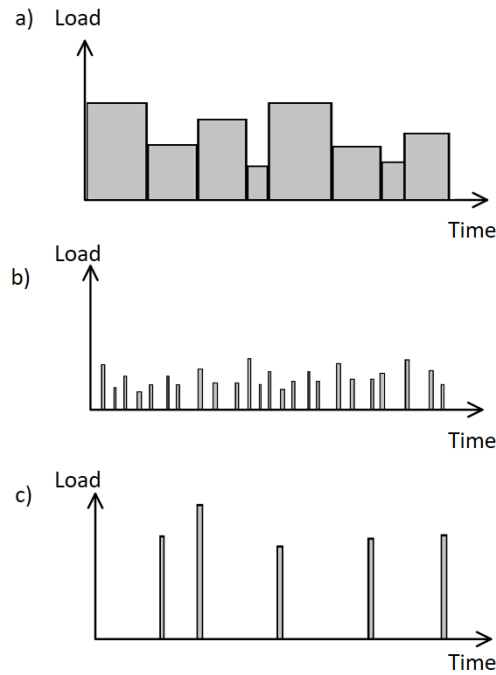


Figure 2.3: The time variability of the magnitude of the load after CIB (1989)

According to the Joint Committee on Structural Safety (JCSS, 2001) imposed loads can be divided into the same two categories as CIB mentions: *sustained loads* and *intermittent loads*. The sustained loads were depicted in the same manner as CIB and are based on ordinary load situations, such as furniture, and the ordinary occupancy of people. JCSS also describes the intermittent loads as more unusual loads that are larger but have a shorter time span. For instance, gatherings of people at an event or party and loads from remodeling or renovation.

2.1.1.2 Categorization based on spatial variation

Imposed loads are divided into two categories according to their *spatial variation*, and these are *concentrated* or *distributed* loads (Isaksson et al., 2011). The *uniformly distributed load* is a load model used in the codes and applied by engineers when they design building structures. This load may not, however, represent the actual load situation in a building. Creating a load model is significantly different from recreating a physical representation of a worst-case load scenario but it is necessary in order to simplify calculations. The *concentrated load* can be depicted as an influence area with the shape of a square and a width of 50 mm (SIS, 1991). the imposed loads can be modelled either by the uniformly distributed load, the concentrated load or a combination of both of these loads. For large concentrated loads at specific points it is important to calculate their local impact, therefore these loads are sometimes calculated separately (SIS, 1991).

2.1.1.3 Values for imposed loads

Eurocode 1991-1-1 states the values for imposed loads by giving a range for the load in different situations. These situations are divided into four different categories, in this study only category A and B will be discussed. This range is shown in table 2.1 below.

Table 2.1: The characteristic values for imposed loads for offices and residential buildings according to Eurocode 1991-1-1

Category	q_k (kN/m ²) uniformly distributed load	Q_k (kN) point load
A: Residential building – floor	1,5 – 2,0	2,0 – 3,0
B: Office sites	2,0 – 3,0	1,5 – 4,5

This range can further be specified in national annexes such as Boverkets building rules EKS 11 (2019). The specified national values for Sweden are given in table 2.2.

Table 2.2: The characteristic values for imposed loads for offices and residential buildings according to the national annex, Boverkets building rules (2019)

Category	q_k (kN/m ²) uniformly distributed load	Q_k (kN) point load
A: Residential building – floor	2,0	2,0
B: Office sites	2,5	3,0

For office spaces in particular many studies have tried to define a space per person benchmark. A survey from the British council offices from 2007 provided a benchmark of 12 square meters per person, according to Haynes et al. (2017). This is a general value relevant for the entire office space, however it shows how much office space goes unused by people. According to the Swedish Work Environment Swedish Work Environment Authority (2021) it is important to have a distance of at least 120 cm to be able to walk past another person in a corridor and a distance of 70 cm to walk past furniture. This could be simplified into a person needing about one to two square meters to be able to walk through a corridor. That would entail one person per square meter as shown in figure 5a. There are, however, situations with higher densities if perhaps there was a group of people sitting at a table for a meeting or standing and talking to each other. A few depictions of the density of people per square meter are shown in figure 2.4.

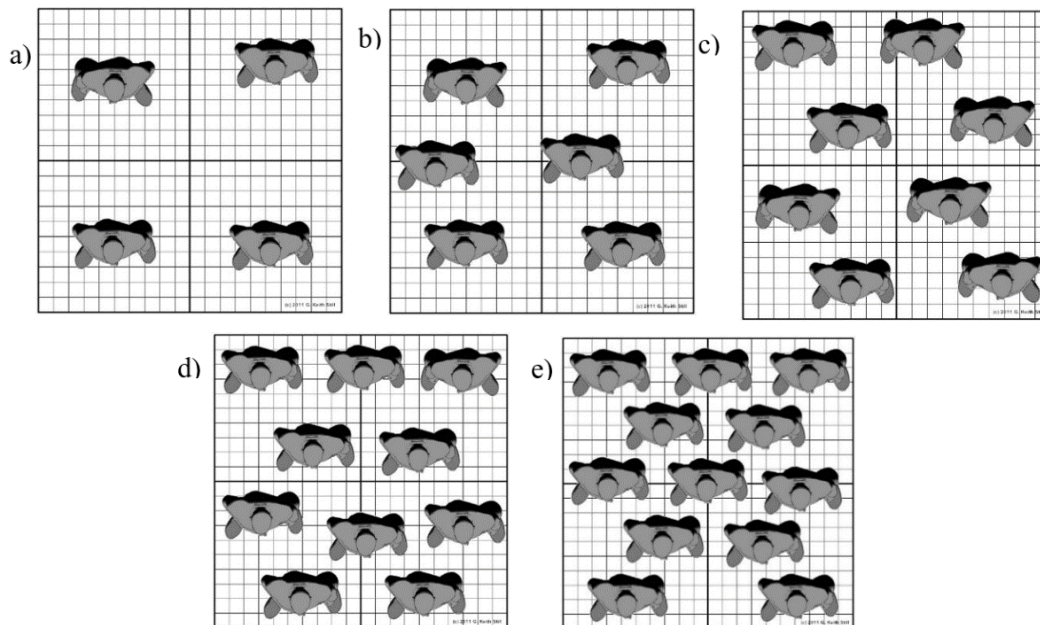


Figure 2.4: a) 1, b) 1,5 c) 2 d) 2,5 and e) 3 people per square meter, with permission from Still (2019).

2.1.1.4 Previous studies on imposed loads

Some previous studies will be discussed in order to have an understanding of imposed loads. Many of these studies state the need for more research which is hopefully something that measurement systems will be able to achieve in the future.

One of the earlier studies on imposed loads was conducted in the 1970s by Lars Sentler. Sentler's report (Sentler, 1975) describes different models that had previously been conducted and draws comparisons between them describing advantages and disadvantages. According to Sentler (1975) the concept of imposed loads was first studied in the 1950's. Sentler (1974) describes two different areas regarding imposed loads: the applied and the theoretical part. The applied referring to information, surveys and tests relating to the actual loads observed in the buildings and the theoretical part referring to an understanding of the concept and the use of different models to represent these loads in a design situation. Sentler continues by stating the need for further studies in both areas.

Since Sentlers studies, other studies have been conducted such as the study by CIB (1989). CIB (1989) states that the information gathered in the surveys that Sentler and another study present are difficult to transfer into a form that is available for general use. They continue by stating that the sustained loads are more investigated than intermittent loads where there is very little information available.

A publication from Honfi (2014) on serviceability floor loads has drawn the conclusion that there is a lack of consistency in the load models according to the structural design codes (Eurocode) and the probabilistic model code (JCSS, 2001). This inconsistency is present in the maximum loads, combined effect of actions as well as the expected duration of loads. A significant issue which was raised was the inadequacy of the stochastic models which in turn is due to a limited number of surveys and empirical data representing the actual loads in buildings. The existing surveys are also limited and do not take all aspects into account such as the duration of extraordinary loads, which is the same as the intermittent loads seen in figure 3b. Another limiting aspect is that the structural codes are often based on the ultimate limit state which can lead to conservative or non-conservative loads in serviceability. Unfortunately, this is somewhat a necessary restriction due to the need for a certain level of simplicity in design codes (Honfi, 2014).

A previous study conducted at Lund University has studied the value of the characteristic imposed load (Bengtsson and Sandberg, 2020). Four different offices in southern Sweden were studied. In the study a load survey was conducted by weighing different objects within the offices to create a probability model to find the variations in the characteristic value. The conclusion of the study was that the value used in the Eurocode 2-3 kN/m² is somewhat conservative as the values that were found were closer to 1,5 kN/m². Furthermore, it is somewhat unclear what the basis for the value 2-3 kN/m² in Eurocode is. The study also concluded that there are still some uncertainties regarding both the load studies and load models related to imposed loads. Another relevant conclusion was that intermittent load has the largest uncertainties.

2.1.2 Dynamic loads

According to Eurocode (SIS, 1990) imposed loads should be considered as a quasi-static action, which can be depicted as very low-velocity impact. According to Eurocode it is acceptable to include dynamic loads in the load model as long as no resonance occurs. Most of the loads that will affect the slab will be quasistatic with occasional dynamic loads created by larger gatherings such as parties. In buildings where these types of large dynamic loads often occur for example at a gym, special dynamic analyses may be required (Eurocode 1991).

According to Eurocode loads can be considered with the help of “static values or by applying *equivalent dynamic amplification factors* to the static actions” (SIS, 1990). The equivalent dynamic amplification factor is the ratio between the dynamic and quasistatic response. There is little information on the dynamic loads that affect residential buildings or office buildings presented in Eurocode. This is probably due to the relatively small load that regular human usage creates, even the intermittent loading as mentioned previously often has such a short duration that its effects are minor. Eurocode 1991 describes how the *equivalent dynamic amplification factor* also known as the *Dynamic magnification factor (DMF)* can be used for forklifts which can give an idea as to how a factor could be created for large dynamic actions in residential buildings.

2.2 Timber structures

Timber has been used in building structures for centuries. Timber also has the advantage of a very broad usability, it can be used structurally for floors, roofs, walls, columns, beams and more. Timber can also be used to achieve aesthetic goals, such as in façades and furniture. In recent years timber has found new popularity due to its advantages as a sustainable material. Timber can be adapted in different ways such as plain timber beams, glue laminated beams and cross laminated timber (CLT) slabs. In this study the focus will be on CLT slabs. Unfortunately, timber structures are particularly sensitive to high imposed loads as they are relatively light in relation to the magnitude of the imposed load itself, therefore timber is of particular interest in this study.

When measuring the strength of wood, the values often vary depending on the direction of the fibres. This is due to the anisotropic nature of wood as a material, meaning that the properties vary in each direction. To be concise wood is an orthotropic material, meaning its properties vary in three different directions, the longitudinal (L), radial (R) and tangential (T) direction as seen in figure 2.5. The radial and tangential directions are often very similar in strength, therefore these directions are often classified in the same manner using the joint term strength perpendicular to the grain (Shmulsky and Jones, 2019).

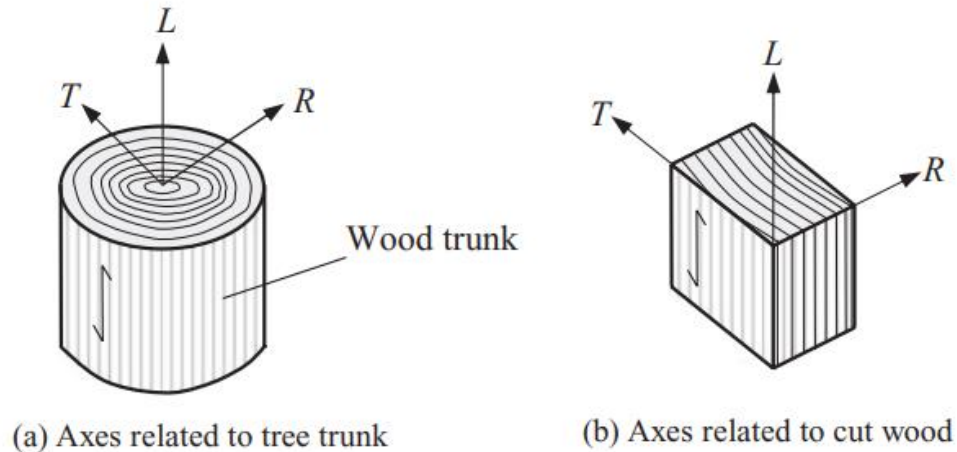


Figure 2.5: Image depicting the different axes in wood, with permission from Shmulsky and Jones (2019)

2.2.1 Timber grading

Wood grading is an important aspect in this study due to the impact an incorrect grading can have on the amount of timber that is being efficiently used. The more accurate the strength of the slab in relation to the given design values the more efficiently the material can be used.

Grading of the quality of wood can be accomplished with different methods. The oldest method is *visual grading*, which is most often based on the grading of knots (Blaß and Sandhaas, 2017). Visual grading is performed by using the maximum knot area ratio, which is the ratio of knot area to the remaining area of wood. The maximum knot area ratio then indicates a specific strength class. Visual grading is performed by humans which leads to a human error factor and ambiguity in the results. Other aspects that can be used in visual grading are: slope of grain, cracks, reaction wood, fungi and insect attack, discolorations and curvatures (Blaß and Sandhaas, 2017).

Today *machine grading* is more popular, it is primarily based on the measurement of the dynamic MOE via vibration. The dynamic MOE is similar to the MOE in the sense that it is also the ratio of stress to strain, but it differs since it is measured under vibratory conditions. It is advantageous to use the dynamic MOE in grading situations since it correlates better with strength than knots. Machine grading is a newer technique which was developed in 1960 (Blaß and Sandhaas, 2017) and has grown in popularity in correlation with the increasing demand for wood. Other advantages with machine grading are the accuracy of the measurements and the reproducibility of the grading. Machine grading can also encompass optical methods such as surface scanning and x-rays for knots. The optical method results in knot grading which is often combined with the grading of the dynamic MOE to obtain an even more accurate measurement (Blaß and Sandhaas, 2017).

Modulus of Elasticity

The modulus of elasticity is one of the most important values in reference to the strength of timber, it is a measurement of the materials elasticity and is based on the ratio of the tensile stress to the tensile strain. When considering the bending of the slab, which is a structural element consisting of a flat, horizontal surface, there are two different ways the slab can bend, either parallel to the grain or perpendicular to the grain. Loading perpendicular to the grain can lead to both types of bending. Figure 2.6a depicts bending parallel to the grain, which is the same as the slab bending in the longitudinal axis. Figure 2.6b depicts bending perpendicular to the grain which can be either in the tangential or radial direction, as mentioned previously these axes have similar properties and are therefore grouped together in the term perpendicular to the grain. When considering the modulus of elasticity, a statistically based value is often used, the mean value. Two important values when measuring bending are the mean *modulus of elasticity* (MOE) perpendicular to the grain ($E_{m,90,mean}$) and parallel to the grain ($E_{m,0,mean}$). The MOE parallel to the grain is much higher than perpendicular to the grain. Other important values are the MOE in tension and compression both perpendicular to and parallel to the grain. Another aspect is the characteristic strength in bending, compression, and tension both perpendicular and parallel to the grain.

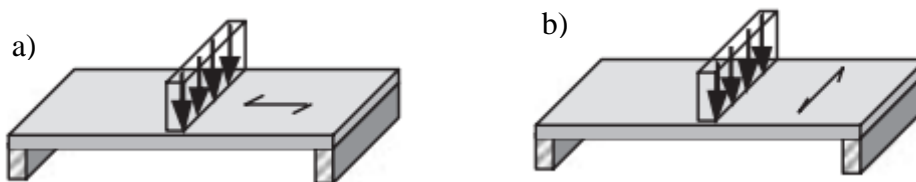


Figure 2.6: Image depicting a slab subjected to a) bending parallel to the grain and b) perpendicular to the grain where \longleftrightarrow depicts the grain direction. This figure was used with permission from Porteous and Kermani (2007)

2.2.2 Cross laminated timber (CLT)

Cross laminated timber (CLT) will be used in this study due to it being a relatively new environmentally friendly material which has not been investigated to the same extent as other building materials. CLT was first produced in the 1990s by leading universities searching for a way to minimize the use of concrete. In order to do so researchers tried to find a way to optimize the use of timber, they did this by placing multiple timber beams in layers perpendicular to each other. Timber as mentioned previously is strongest in the longitudinal direction, by layering the timber perpendicularly the researchers were able to make use of the strongest parts of the timber in both directions and thereby create a much stronger material than just timber. This leads to CLT having excellent strength and stiffness properties and also allows it to easily be glued into different shapes and sizes. Some other advantages with CLT are that it forms a climate-smart carbon sink in structures and is a renewable and sustainable building material. There are also health benefits from using CLT. Research has found that people sleep better in rooms made of wood due to the materials ability to “breathe” and maintain an active relationship to the relative humidity (Swedish Wood, 2019).

Structural components made of CLT are primarily used for walls and floor structures. Both structural components require robustness and must be able to carry the loads they are subjected to. For floor structures it is of particular importance to achieve stability and vibrational and acoustic comfort. There are also specific requirements regarding deformation, vibration, fire safety, acoustic insulation and thermal insulation. When fulfilling these requirements, it is important to consider alteration such as altered weight, appearance and strength. A floor structure is made up of a surface layer, a separating layer and a load bearing layer. There are different types of CLT structural systems, which stand for the load bearing layer. In this study the flat floor structure which consists of the CLT panel alone is of primary interest, seen in figure 2.7. The strength can vary depending on the amount and thickness of the layers and the strength class of the timber in each layer. The most common design for CLT is to utilize the strongest direction of the timber in the main span direction, so that the fibres are parallel to the main span of the slab, as seen in figure 2.7. CLT slabs can achieve spans of up to five meters (Swedish Wood, 2019).

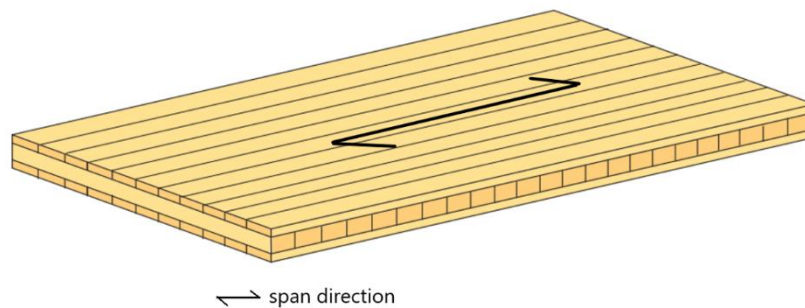


Figure 2.7: A depiction of a CLT flat floor structure. The figure is used with permission from Swedish Wood (2019) and is taken from the CLT Handbook.

There are two other types of timber CLT slabs: hollow floor structures and cassette slabs (Swedish Wood, 2019). Cassette floors are created by gluing glulam joists to the underside and top of the slab which leads to a larger capacity for loads and longer spans, as seen in figure 2.8a. Cassette floors often have a hollow center which can be used for insulation, both heat and acoustic. A way to further improve the acoustic insulation is to not fully connect the floor structure and the sub ceiling which prevents the sound from travelling between floors. The other type of timber slabs are hollow floor structures which are not as commonly used in Sweden. In hollow floors the top and bottom slab are joined with spaced web joints, seen in figure 2.8b. Just as for cassette floors this allows for insulation between the top and bottom floor. Another type of timber slab is the composite slab where timber is combined with another building material for example concrete, although other materials can be used. There is a wide variety of composite slabs but they will not be mentioned further in this study (Swedish Wood, 2019).

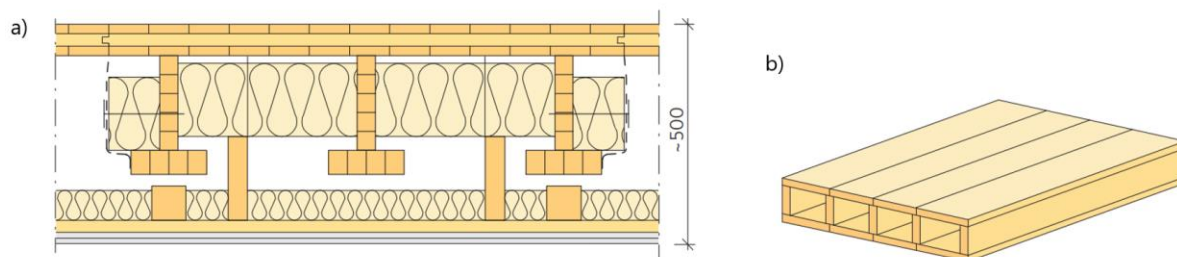


Figure 2.8: a) A cassette slab with a suspended ceiling, which is made with a CLT slab reinforced by web joists and flanges. b) A hollow core slab. The figures are used with permission from Swedish Wood (2019) and are taken from the CLT Handbook.

2.2.3 Sustainability

Given the effects of climate change on the world, sustainable buildings and building materials are ever-growing concerns. This study aims to address this by looking at improving measurements of imposed loads to both conserve and better use the sustainable timber materials that are available, such as CLT slabs. In comparison it is well known that concrete stands for a large percentage of the environmental impacts from the building sector and is not a renewable resource. By using alternative materials such as CLT the impact from concrete can hopefully be minimized. When assessing the environmental impact of a material it is important to include the materials entire life cycle, which includes: the raw materials extraction; processing and conversion; usage and the disposal of the material. This is why the renewability of timber is so important because it will naturally decompose faster and will also regenerate much faster than for example a cement quarry.

An example of the benefit of wood regarding energy, is the amount of energy that can be saved when building with wood in comparison to concrete. The amount of energy required for the material and building of a wall made of concrete building blocks with no insulation compared to a wall made of plywood siding with no sheathing is nearly 10 times more (Shmulsky and Jones, 2019). Energy usage can lead to further emissions that will increase the global warming and lead to further consequences for the environment. The carbon dioxide emissions can also be compared, where results show that an all-wood construction on a concrete foundation required only 35 % as much energy and nearly a third as much release of carbon dioxide as a steel construction on a concrete foundation (Shmulsky and Jones, 2019).

Another aspect to consider when looking at the environmental aspect of using wood as a building material is the fact that raw material demand is growing. To satisfy the demand in a sustainable way wood may be the solution. However it is also important to take into account the preservation of wildlife sustainability and the biodiversity within the forest when acquiring wood (Shmulsky and Jones, 2019).

2.3 Structural health monitoring

Structural Health Monitoring (SHM) may be one of the future uses of this study: by ascertaining the accuracy of measurement systems it can be considered as more relevant to implement sensors in buildings over a longer time. This technique has already been implemented in larger structures such as bridges. SHM can be defined as the process of

implementing a damage identification strategy, where damage can be defined as changes to the structural system (Farrar and Worden, 2007). By finding the damage it can be possible to repair the damage, prevent the damage from worsening or to remove the structure to prevent any accidents. SHM has become increasingly popular in recent years due to the potential safety and economic benefits that this method and the technology may result in. Another reason for the increased interest is the fact that many civil structures are approaching or exceeding their initial design life (Farrar and Worden, 2007). To be able to continue using these buildings, testing their ability and fixing small faults may lead to longer design lives and lead to a higher level of understanding of this type of building. An example of a construction that would have greatly benefitted from some SHM is the Morandi Bridge which collapsed in 2018. The collapse was attributed to poor maintenance and construction flaws (Pianigiani, 2020). The collection of data from SHM can not only be used for maintenance but also provides some insight concerning the loads to which the structure is subjected.

2.3.1 Bridge Weigh in Motion (BWIM)

Bridges are an example of a large structure that SHM can be conducted on. Finding a load that is the equivalent to imposed loads for buildings is slightly more challenging in bridges due to the larger loads and load variations. With the help of so-called bridge weigh in motion (BWIM) systems axle loads from heavy traffic can be collected at a specific bridge location. This system essentially utilized the bridge as a scale providing measurements of the traffic loads using strain gauges attached to the short span bridge. The systems are designed to weigh the axle and gross vehicle loads while a vehicle is in motion. This is much more efficient than static scales which require the vehicle to be stationary when weighing. By using the collected data from BWIM, a distribution function for the extreme loads can be created, unfortunately this is quite challenging for bridges due to the incredibly large loads that they are exposed to. In a study carried out by Fredrik Carlsson, three different methods were used to ascertain the traffic load's natural variation (Carlsson et al., 2007):

- Place different loads along an influence line or area to be able to calculate the average forces.
- Decide on stochastic values that describe the loads from vehicles and simulate fictive vehicles that can be used to decide the average load on bridges.
- Create theoretical models of vehicles and from the models calculate the average force.

An example from Fredrik Carlsson is to use influence lines to calculate the maximum moment. Carlsson did this by placing the load of a vehicle on a simply supported beam. Due to the vehicle having two axles, two point loads are depicted as seen in figure 2.9. With this basic model, Carlsson proceeds by gradually moving the axle loads to find the position that leads to the maximum moment (Carlsson et al., 2007).

A similar method is used when calculating the deflection that occurs due to two vehicles meeting each other on a bridge. In Carlsson's study the dynamic affects can be quite large and the static affects are also of a different load class than those used in buildings therefore the need for such models is much larger in the infrastructure sector in comparison to buildings. Creating a simulation for human activity within a building could potentially be modeled in a similar way (Carlsson et al., 2007).

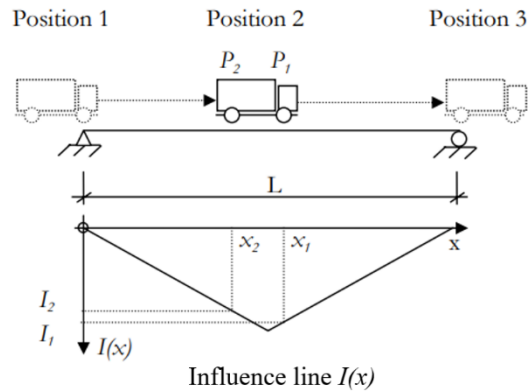


Figure 2.9: An illustration depicting the average forces from a single vehicle and how they can be calculated. The figure was used with permission from Carlsson (Carlsson et al., 2007).

2.4 Measurement systems

Measurement systems will be used in the test to calculate the load on the slab. There are many different types of measurement systems and they can be divided into three categories:

- Sensors or transducers which are the receiver of the information,
- Intermediate processors which convert information or process signals and
- Output devices, which transmit the results.

This report will discuss measurement systems but will focus on the use of different types of sensors and transducers. There are a few differences between sensors and transducers. Firstly, the sensor is often the smallest unit, in comparison to the transducers which often contain a sensor, wiring connections and sometimes the signal processing. Sensors can also be described as the item that the measurand directly influences. The measurand being the quantity that needs measuring. The influence detected by the sensor can then be translated with the help of a transducer into an electric signal. In other words the transducer is “the device that enables the correspondence between input and output” according to Stefanescu (2011).

Sensors can be used for monitoring different characteristics of a structure. The different types of monitoring can be safety monitoring; usage monitoring, for example measuring the strain; health monitoring to find out the structure’s current state and deterioration monitoring for predicting future outcomes. An optimal sensor is stable, reliable, and able to consider the environmental effects such as humidity and temperature. These are of particular importance when it comes to timber structures due to their sensitivity to humidity. Important points to consider when choosing sensors are: the measurands, the quantities to be measured; the placement of the sensor and the accuracy needed (Chen and Ni, 2018).

2.4.1 Measurands

There are three different measurands of primary interest for static monitoring which will be conducted in this study. The first is displacement, the second is load and the last measurand is strain. There are other measurands such as acceleration that are more relevant for dynamic actions, but these will not be considered.

The *load* is the value that is of primary relevance in this study. Therefore, discussing methods for directly measuring the load is of interest.

Displacement is an important measurand of imposed loads, which can be due to dynamic and quasistatic components and variations of static loading. Displacements are often relative values and require reference information (Chen and Ni, 2018). Dynamic displacements from vibrations can be calculated from the acceleration of the object.

The *measured strain data* can be used to calculate stress and find the forces acting on the structure. A variety in temperature can greatly affect the result of the strain and there are some self-temperature compensating sensors that can be implemented where there are large temperature variations. When determining the total strain value a baseline value is required otherwise only the differential strain can be measured (Chen and Ni, 2018). To be able to convert strain into other values such as stress and loads it is important to know the position of the acting force. The position of the acting force must also be constant and the structure should only have linear deformation (Cardei et al., 2021).

2.4.2 Types of measurement systems

There are many different types of measurement systems. This study will mention the following types of sensors: Linear Variable Displacement Transducers (LVDT), strain transducers, strain gauges, potentiometers, fiber Bragg grating sensor (FBG), load cells and Laser Doppler Vibrometers (LDV). Two of these sensors will be tested in this study: the potentiometer and the strain gauge.

Today there is a substantial availability of high-quality technology but for realistic testing the economic factor must be considered. Therefore, optical and wireless technology will be excluded in this report, despite the potential advantages in measuring accuracy. Sensors can be divided into two categories: either electrical or optical fibers. Sensors using electrical fibers can be disrupted by external electromagnetic field disturbances, while optic fibers are not sensitive in the same way since they are made by light signals. Optical fibers are also smaller and more lightweight, can withstand high temperatures and are more robust in the presence of aggressive chemicals (Mitschke, 2016).

2.4.2.1 Potentiometers

A potentiometer converts a longitudinal movement into an electronic quantity of the same proportions (Variohm, n.d.-c). The potentiometer is a position sensor and measures the displacement along a single axis, in this study the displacement will be measured by the CLT slab pushing down on the potentiometer. The potentiometer is a contacting type of sensor meaning that the moving parts must make contact during use. Some advantages of the potentiometer are its robustness and inexpensiveness in comparison to other non-contact sensors. Potentiometers also have a long life.

The potentiometer that will be used in this study is a linear potentiometer with spring return function SLPS-75-D-5K-1M produced by Opkon (n.d.) shown in figure 2.10. According to Opkon the potentiometer has a linearity error of $\pm 0,2\%$ for 75-100 mm and $\pm 0,5\%$ for <75 mm and a measuring range of 10-100mm. The linearity error is the deviation of the measurement values from the curve of the expected results. The product information also states that there is a repeatability error of $<0,01$ mm.



Figure 2.10: Depiction of the potentiometer used in the test from (Opkon, n.d.)

2.4.2.2 Strain gauges

There are many different types of strain gauges such as foil strain gauges and wire strain gauges. Strain gauges are an inexpensive choice and quite small which allows for more specific placement in different areas (Chen and Ni, 2018). A disadvantage with strain gauges is that the application itself is quite important. Due to the need for a precise application the strain gauges are quite sensitive measurement systems. Strain gauges are produced with no protection and are therefore sensitive to the natural elements if placed outdoors, which is also a disadvantage. The fact that the strain gauges must be individually placed means that they can rarely be reused. Metal strain gauges often have a gauge factor of about 2, the gauge factor can be defined as the fractional change in resistance per unit strain. This means that the sensitivity of metal strain gauges can be 10^{-6} strain (Bajpai, 2018).

For measuring wood with a strain gauge the recommended length is 10-20 mm according to Tokyo Measuring Instruments Lab (n.d.-a) since wood has a low elastic modulus. When measuring a structural timber element, the aim is to find the overall strength. For wood as a material, it may be of more interest to find the strength in one area. Therefore, when measuring structural timber it may be of more interest to use a larger strain gauge. Previous studies have used different lengths. One study on timber deformation (Anshari et al., 2012) used 10 mm strain gauges for deformation, another study (Aicher et al., 2016) used 20 mm and one study (Al Ali et al., 2021) used 60 mm. This shows that although a 10-20 mm strain gauge may be recommended for wood it is also possible to collect reliable results with other lengths.

In the test a single axis polyester strain gauge with the length 60 mm and width 1 mm as depicted in figure 2.11, will be used. According to the product information (Tokyo Measuring Instruments Lab, n.d.-b) the strain limit is two percent (20000×10^{-6} strain).



Figure 2.11: Figure of the strain gauge used in the tests, the figure was used with permission from Tokyo Measuring Instruments Lab (n.d.-b)

2.4.2.3 Linear Variable Displacement Transducers (LVDT)

The Linear Variable Displacement Transducer also known as a Linear Variable Differential Transformer “is a displacement sensor that measures physical movement and represents this change as an output voltage” (Misra et al., 2014). Advantages with the LVDT are its high resolution and precise measurements, it also has a long life-span due to its friction free operation. The LVDT is also highly sensitive, responsive, and robust. The disadvantages of an LVDT are that it requires calibration. This calibration can easily be affected by human errors and environmental conditions. Faulty calibration may also lead to non-linear results leading to low accuracy (Misra et al., 2014). An example of an LVDT is ACT1000A from (Elkome, 2016). According to the product information from Elkome the measuring distance is ± 25 mm with a linearity error of $\pm 0,05\%$.

In comparison to the potentiometer the LVDT is slightly more precise when measuring small deformations and is also limited to measuring smaller deformations. If the LVDT were to be used in this study it would be most efficient to measure the strain parallel to the slab. This could have been done by measuring the deformation of the slab in the load bearing direction and then calculating the strain by comparing the length difference with the total length of the slab.

2.4.2.4 Strain transducers

As mentioned previously a sensor is the item that the measurand directly influences. In this case the strain gauge is an example of a sensor because it creates the first conversion of the measurand. Strain transducers are often made up of a Wheatstone bridge, which in turn consists of four strain gauges that are bonded together on a silicon chip. The strain gauge detects the elastic deflection which leads to resistance changes, which the Wheatstone bridge measures (Stefanescu, 2011).

An advantage of strain transducers is that they can be easily applied by simply screwing them onto the object that is to be measured. In comparison to a strain gauge which requires precise



Figure 2.12: A depiction of the ST350 Strain transducer with permission from BDI (n.d.).



Figure 2.13: A depiction of the ST350 Strain transducer from BDI (n.d.) in use.

application often performed by a professional. Another advantage with the strain transducer is the fact that the strain gauges are placed inside a protective layer and therefore have no need for extra placement of protection from weather and other environmental factors (BDI, n.d.). An example of BDI's ST350 Strain transducer is shown in figure 2.12 and a figure of the strain transducer is shown in figure 2.13.

2.4.2.5 Fiber Bragg grating (FBG)

The FBG is a microstructure, it consists of a fiber with a length of a few millimeters and a coated diameter of 250 micrometers. The light then travels within the core of the fiber. When using an FBG as a strain sensor, which would be the relevant use in this study, the fiber will stretch and compress in order to measure the strain. When the fiber is deformed changes in the period of the microstructure and the Bragg wavelength occur (HBM, n.d.-c). An example of a patch strain sensor using FBG technology is shown in figure 2.14. It has a strain measurement range of $\pm 20000 \mu\text{m/m}$.



Figure 2.14: FS62PSS Patch strain sensor. The figure is used with permission from HBM (n.d.-a)

Due to its small size and fast response Fiber Bragg grating (FBG) technology is one of the most predominant types of systems used within fiber optics (Sahota et al., 2020). FBG sensing has gained popularity due to its small size, fast response and distributed sensing. All fiber optic systems share an immunity to changes in the electromagnetic fields.

Load cells

Load cells are measurement systems that measure loads. There are several different types of load cells: mechanical; strain gauge-based and others, such as fiber optic and piezo resistant. Most load cells today are based on strain transducers (Chen and Ni, 2018). One disadvantage of load cells is that the area of the load cell is limited, large elements used in structural engineering such as beams might not fit on the load cell and the load cell will therefore be hard to use. The accuracy of load cells varies and can have an error of 0.0116% up to 0.0230% according to Variohm (n.d.-b). Figure 2.15 shows an example of a single point load cell.

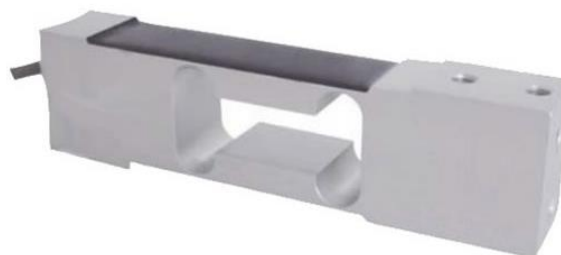


Figure 2.15: Example of an AL6N single point load cell. The figure is used with permission from Variohm (n.d.-a)

2.4.2.6 Laser Doppler Vibrometers (LDV)

The LDV functions by sending out two beams of light, one is a reference beam and the other a measurement beam. The measurement beam is sent to the object where the light waves are slightly altered and then reflected to the measurement device. The measurement device then compares the reflected beam to the original reference beam and by comparing the two beams the vibration frequency is found which is used to calculate the displacement of the test object. According to Polytec (n.d.-a) laser doppler vibrometry is currently the best method for measuring displacement and velocity resolution. One advantage of the LDV is that it can be used for places that are hard to access. The LDV does not need to be connected to the test object which is an advantage for small test objects and minimizes any potential side effects that a load placed on the test object could induce. The LDV can also measure both short and large distances (Polytec, n.d.-a).

An example of an LVD is the Rotational Laser Vibrometer, RLV-500, from Polytec (n.d.-b) shown in figure 2.16. The RLV-500 can achieve a resolution of 2 nm when measuring the deformation (Polytec, n.d.-a).



Figure 2.16: The Rotational Laser Vibrometer RLV-500 with permission from Polytec (n.d.-b)

2.4.3 Placement of the measurement systems

To understand how the measurement systems are to be implemented in this study an analogy could be drawn between the CLT slab and a scale. When a person, furniture or other load is placed on the slab, it functions as a scale and can, with the help of the implemented measurement systems, provide the loads from the different items. In order for the measurements to be as accurate as possible the position for the measurement systems on the slab should be given due consideration.

2.4.3.1 Previous studies

A few previous studies using measurement systems will be discussed to find an optimal placement of the measurement systems. The study conducted by Anshari et al. (2012) consisted of multiple different tests using measurement systems, the test on short glulam beams will be presented here. First of all it is important to note that there are some differences between glulam and CLT beams. Despite this it is assumed that there are enough similarities to use a similar set up for the CLT slab in this study.

In the test on short glulam beams Anshari et al. (2012) used one displacement transducer and seven strain gauges in total. The displacement transducer was a CDP-25 and the strain gauge was PFL-10-11 (Tokyo Sokky Kenkyujo Co. Ltd.). Four strain gauges were placed at the mid span and three were placed 130 mm from the middle. The displacement transducer was placed at the mid span underneath the beam. This is shown in figure 2.17.

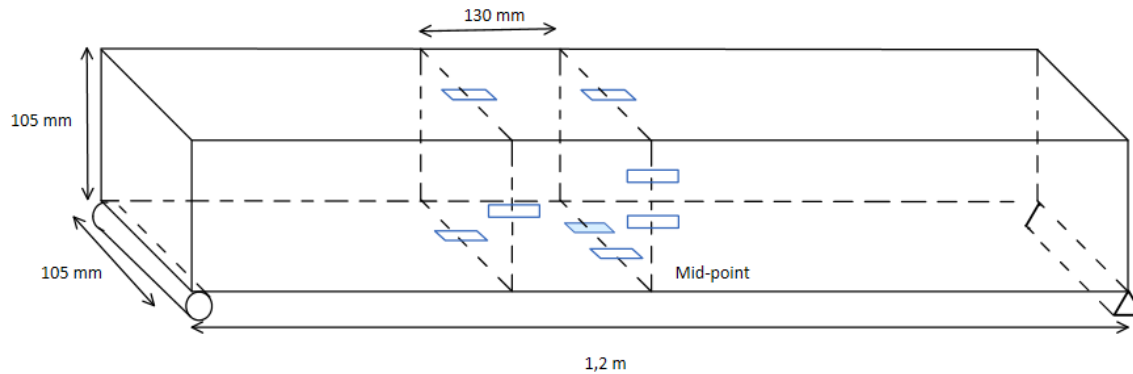


Figure 2.17: The placement of the measurement systems depicted on the short glulam beam after Anshari et al. (2012). The rectangular outline depicts the strain gauges, and the shaded rectangle depicts the displacement transducer.

Aicher et al. (2016) also conducted a study on measuring the deformation of a CLT-slab with the help of measurement systems. In that study strain gauges were placed in the middle of the beam and two triaxial strain gauge rosettes were placed between the middle of the beam and the supports. The triaxial strain gauge rosettes will not be elaborated upon since they are not covered in this study. Six strain gauges were placed in the middle of the beam three on the top and three on the bottom which is depicted in figure 2.18 below. When placing the strain gauges they were glued onto the slab at least 15 mm from the edge and in order to avoid defects and cracks the strain gauges were sometimes placed further in but they were never moved than 60 mm.

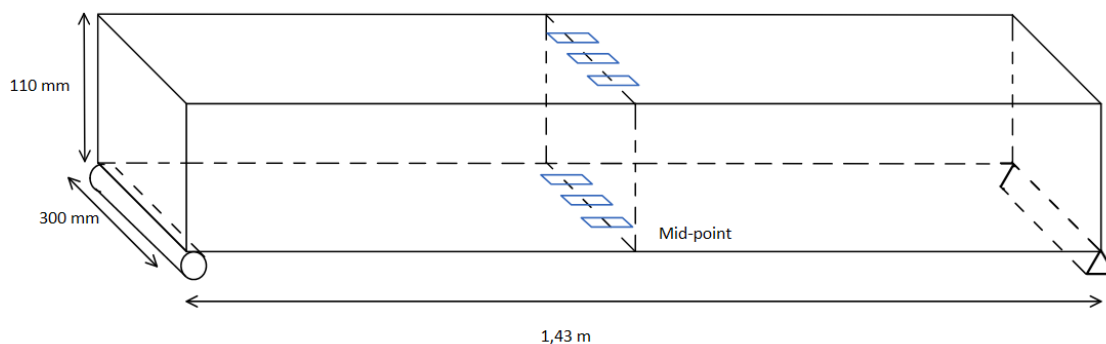


Figure 2.18: placement of measurement systems according to Aicher et al. (2016)

3 Method

The execution of the tests will be explained in this chapter. First the material needed will be described, followed by the analytical method and finally the execution of the test. Simplifications and assumptions will be stated.

3.1 Material

The primary material for this test is the CLT slab. The chosen measurement systems are potentiometers and strain gauges.

3.1.1 CLT slab

The same CLT slab that will be used for all the tests and it is a CLT 90 C3S NVI (Storaenso, 2017), with the original dimensions 90x1850x2950 mm (Storaenso, 2017). In this case the slab had been roughly divided in the middle of the width since it had been used for other experiments. The panel type is C3s meaning the slab consists of 3 layers. The slab has the standard NVI, which stands for non-visual quality. The grain direction of the cover layer is parallel to the span direction. The thickness of each layer is 30 mm resulting in a total thickness of 90 mm. After dividing the slab, the length was 950 mm and the width was 920 mm. The dimensions for the slab are shown in figure 3.1.

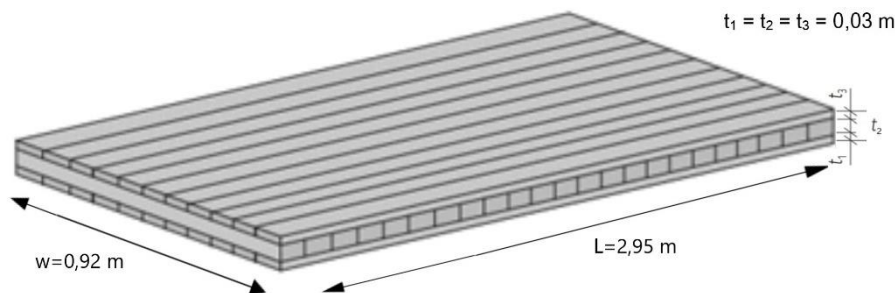


Figure 3.1: Dimensions of the slab.

The quality of the timber is C24 and according to EN 338 the Swedish standard for structural timbers strength classes, a maximum of ten percent C16 is permitted (Storaenso, 2017). The fact that some of the timber can be of a lower class may lead to a lower strength value than that which is given for C24. To simplify calculations only C24 will be used, and strength difference due to the permitted amount of C16 will be disregarded. Some important values that will be needed are listed below.

- The mean modulus of elasticity parallel to the fibers $E_{m,0,mean}=11000\text{ MPa}$
- The characteristic bending strength parallel to the fibers $f_{mk} = 24\text{ MPa}$

The characteristic bending strength will be used for some of the calculations in test 1. This is not representative for an experiment since the characteristic bending strength represents the 5th percentile, i.e. 95 percent of specimens would have a bending strength greater than this value. The mean value for the bending strength can be determined based on the characteristic value

and based on information acquired in e.g., a probabilistic model code (JCSS, 2001). In the case of a timber beam, this can be 50 % greater than the characteristic value while for a glue laminated beam, the relative increase is 30 % greater. A cross laminated timber slab is likely somewhere between these two values. Despite the mean value being more accurate the characteristic value will be used for test 1 in order to prevent any risk of cracking the slab.

3.1.2 Placement of the measurement systems in this study

The potentiometer that will be used in this project is a linear potentiometer with spring return function SLPS-75-D-5K-1M produced by Opkon (n.d.) as mentioned previously in chapter 2.4.2.1. The potentiometer was placed next to the slab in a central position. In order to measure the deformation two metal corner braces were placed on the side of the slab. Figure 3.2 shows the placement of the potentiometer.

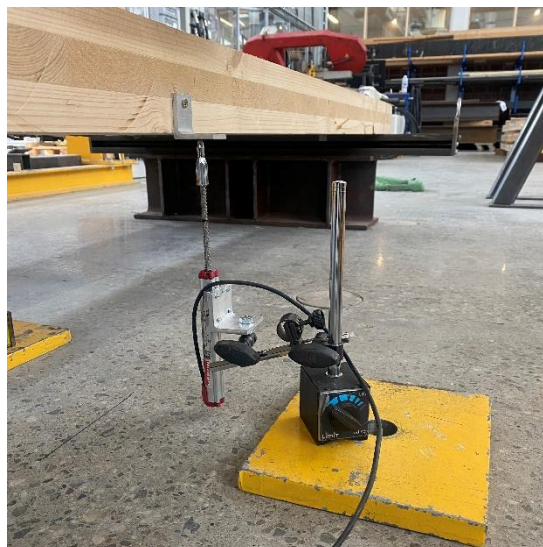


Figure 3.2: The placement of the potentiometers for the test.

In order to place the strain gauge, it had to be glued into place on the timber slab with an adhesive such as a two-component epoxy glue which was used in this case. Before applying the adhesive, the surface was sanded down to create an even surface. Once the strain gauge was glued in place the wires that are faintly seen in figure 3.3 were then soldered on to cables that were led into the QuantumX Data Acquisition system from HBM (n.d.-b).

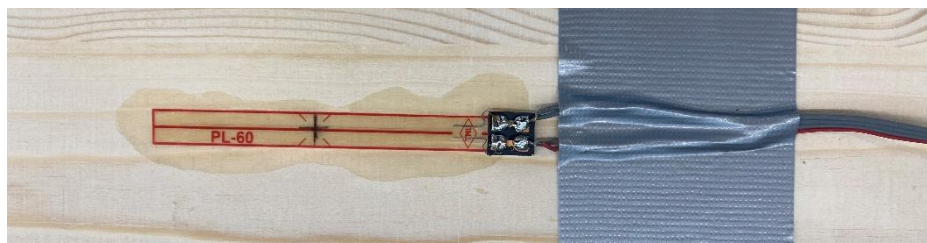


Figure 3.3: The placement of the strain gauge for the test.

Figure 3.4 shows the chosen positioning of the strain gauges, potentiometers and the supports placed on the bottom of the slab. The CLT slab as described in the previous chapter was prepared by applying four strain gauges and two potentiometers (a further figure can be seen in appendix A, figure A.1). The CLT slab was placed on two bearings, one was a roller bearing and the other was a moment-free bearing. The bearings were positioned as shown in figure 3.4. Figure 3.5 shows a further clarifying image of the slab in three dimensions. The roller bearings had a width of 150 mm and were placed 20 mm from the edge. The calculations will be conducted assuming that the length of the slab is determined from the middle of the supports, leading to a slightly shorter slab length of 2,75 m. The measurement frequency for the measurement systems was set to two per second for all the tests.

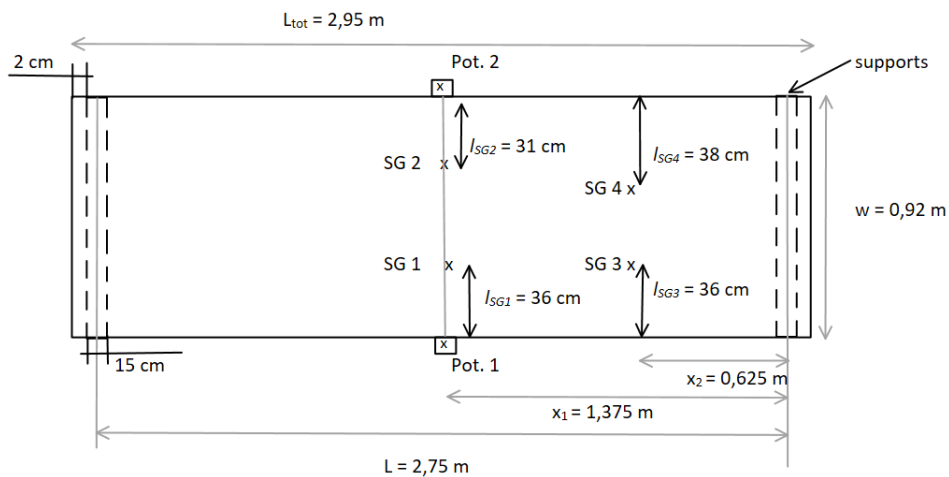


Figure 3.4: The bottom side of the slab with the placement of the measurement systems indicated with SG for strain gauge and pot. for potentiometer.

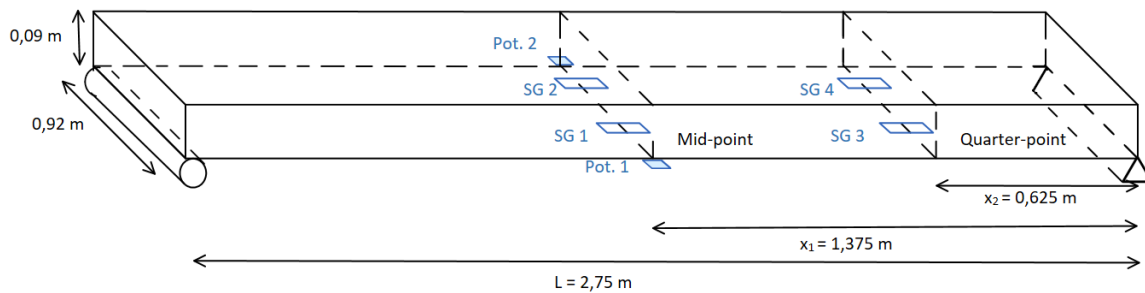


Figure 3.5: A depiction of the entire slab showing the strain gauges placed on the bottom and the potentiometers placed on the sides of the slab.

The middle of the slab is often where the largest deformation occurs therefore two potentiometers and two of the strain gauges will be placed there. Also, according to chapter 2.4.3.1, previous studies have placed measurement systems in the middle of the slab. Two strain gauges were also placed at the quarter point of the entire length of the slab. When the length was shortened due to the placement of the supports the position of the strain gauges was not quite at the quarter point rather further to one side. The reason the strain gauges were placed at the quarter point was to be able to have a greater understanding of the position of the load on the slab.

The strain gauges were also placed at different distances from the slab edge. Originally, they were placed 35 cm in from the slab edge but due to defects or knots seen on the bottom layer

of the CLT at that position the strain gauges were moved further in or out depending on the location of the knot or defect. The strain gauges were not moved more than 5 cm in either direction. Due to the CLT slab having multiple layers it is possible the middle layer and top layer, which couldn't be seen when the slab was upside down, could have contained errors at the point that the measurement systems were placed. The knots and errors in the wood were avoided to prevent the defects from being measured and leading to a lower or higher measured value.

3.2 Analytical method

Timber is designed in the serviceability limit state (SLS) and the ultimate limit state (ULS). In this study the timber slab will be analyzed using Bernoulli Euler's beam theory using the gamma-method which considers the shear flexibility. An alternative method would be to use the Timoshenko beam theory. The two calculation methods are relatively similar in regards to bending stiffness according to Bajzecerová (2017). Since the difference between the methods was so slight the gamma method was chosen in order to simplify calculations.

3.2.1 Load cases

Both the deflection and the strain will be measured and shown in the results. The aim of the study is to determine the differences between the real load on the slab and the load that can be calculated from the measurement systems. Three different types of load cases will be evaluated, a single point load in the middle of the beam, a single point load with varying placement and a uniformly distributed load.

The uniformly distributed load will be calculated to create an approximate load model. The purpose of the load model is to capture the highest response in the system. In this study the load situations used will predominantly be point loads but since the objective of the load model is to find a maximum value it is acceptable that the real load situation is not depicted. The aim with the load model is similar to that of the distribution function Carlsson created for bridge weigh in motion systems mentioned in chapter 2.3.1.

Equations 1-9 represent the three load cases and they are depicted in figures 3.6-8.

Case 1

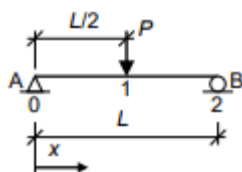


Figure 3.6: Load case 1

$$v_{max} = \frac{PL^3}{48EI} \quad (1)$$

$$M_{max} = \frac{PL}{4} \quad (2)$$

$$M(x) = \frac{Px}{2}, \quad x < \frac{L}{2} \quad (3)$$

Case 2

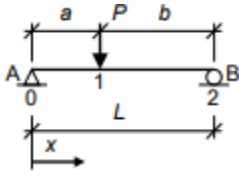


Figure 3.7: Load case 2

$$v_{mid} = \frac{Pa(3L^2 - 4a^2)}{3LEI} \quad (4)$$

$$M^{0-1}(x) = \frac{Pbx}{L} \quad (5)$$

$$M^{1-2}(x) = \frac{Pa(L-x)}{L} \quad (6)$$

Placing the strain gauge at the quarter point requires adjusting the x value for that placement. It is also important to acknowledge the placement of the load which varies in the different tests and used either equation 5 or 6 depending on the placement.

Case 3

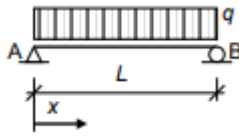


Figure 3.8: Load case 3

$$v_{max} = \frac{5qL^4}{384EI} \quad (7)$$

$$M_{max} = \frac{qL^2}{8} \quad (8)$$

$$M = \frac{qLx}{2} - \frac{qx^2}{2} \quad (9)$$

3.2.2 Deformation calculations

The deformation measured by the potentiometers can be used to calculate the load on the slab. This is done with the help of the load cases mentioned above. Equation 1 for a point load in the middle of the slab, rewritten so as to calculate the load is shown below.

$$v_{max} = \frac{PL^3}{48EI} \rightarrow P = \frac{v_{max}48EI}{L^3} \quad (10)$$

3.2.3 Strain calculations

The moment capacity is calculated according to the equation from Isaksson and Mårtensson (2017) below.

$$M_{Rd} = f_{md}W \quad (11)$$

The equation for the design moment comes from the stress equation which does not have any extra design factors. The equation can be rewritten to calculate the moment as shown below.

$$\sigma = \frac{M_y \cdot y}{I_y} \rightarrow M_y = \frac{\sigma \cdot I_y}{y} \quad (12)$$

The load case for a central point load equation 2 and equation 12 can be used to calculate the point load. To find the maximum load the characteristic bending strength f_y can be used as the stress in equation 13 below. It is important to recall that the mean load which will likely be

found in the experiment is probably 30-50% larger. Despite this the characteristic value will be used for the calculations in test 1 in order to prevent any risk of cracking the slab.

$$M = \frac{PL}{4} = \frac{\sigma \cdot I_y}{y} \rightarrow P = \frac{4M}{L} = \frac{4 \cdot \sigma \cdot I_y}{L \cdot y} \quad (13)$$

Hooke's law, stated below, explains the relation between the stress and the strain when in an elastic state.

$$\sigma = E\varepsilon \quad (14)$$

By inserting Hooke's law into the moment equation an equation based on the strain can be found.

$$M_y = \frac{E \cdot \varepsilon \cdot I_y}{y} \quad (15)$$

By using the moment calculated from the measured strain results a point load can then be calculated, with equations 2 and 15.

$$M = \frac{PL}{4} = \frac{E \cdot \varepsilon \cdot I_y}{y} \rightarrow P = \frac{4M}{L} = \frac{4 \cdot E \cdot \varepsilon \cdot I_y}{L \cdot y} \quad (16)$$

In the same manner as for equation 16 the bending moment for a non central point can be calculated, where x is the distance from the support to the strain gauge. This is calculated from equation 3 and 15.

$$M = \frac{Px}{2} = \frac{E \cdot \varepsilon \cdot I_y}{y} \rightarrow P = \frac{2M}{x} = \frac{2 \cdot \varepsilon \cdot E \cdot I_y}{x \cdot y} \quad (17)$$

3.2.4 Moment of inertia

The moment of inertia (MOI) is an important value in both the strain calculations and the deformation calculations. The MOI itself can be calculated using the dimensions of the slab. This is the simple way of calculating the MOI of a normal beam, called the net moment of inertia.

$$I_{y,net} = \frac{wh^3}{12} \quad (18)$$

For a Cross laminated timber beam, it can be important to calculate the contribution of the deformation from shear, which can be significant. The gamma method according to Annex b for Eurocode 5 (SIS, 1995) can be used to account for this contribution and the effective moment of inertia $I_{y,ef}$ is used for this calculation. The values depend on the reference length l_{ref} which in this case is equal to L , the full span length due to the slab being simply supported. The Steiner's theorem can be used where each object is a Steiner part, in this case the layers of the slab are the Steiner parts and their value shall be reduced by a gamma value depending on their distance to the middle of the slab. An example of a CLT panel with three layers and the

values needed to calculate the moment of inertia using the gamma method are shown in figure 3.9.

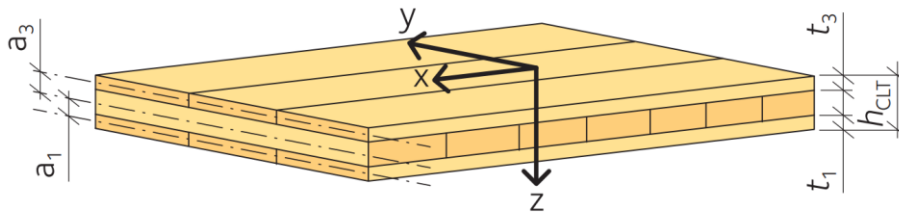


Figure 3.9: Description of values used in the calculations for the moment of inertia. The figure is used with permission from Swedish Wood (2019) and is taken from the CLT Handbook.

$$\gamma_1 = 1 \quad (19)$$

$$\gamma_3 = \frac{1}{1 + \frac{\pi^2 E_{x,3} t_3}{l_{ref}^2} \cdot \frac{t_2}{G_{9090,2}}} \quad (20)$$

The mean value of modulus of rolling shear $G_{9090,2}$ is 50 MPa for CLT panels with only C24 according to Swedish Wood (2019).

$$a_1 = \frac{t_1}{2} + \frac{t_2}{2} \quad (21)$$

$$a_3 = \frac{t_1}{2} + t_2 + \frac{t_3}{2} - a_1 \quad (22)$$

$$I_{ef} = \sum \frac{bt_i^3}{12} + \gamma_i bt_i a_i^2 \quad i = 1, 3 \quad (23)$$

The calculated values for different moments of inertia are shown in table 3.1. These different moments of inertia are used to calculate the maximum possible point load in the middle of the slab. This is done so as to know what load the slab can be loaded to without cracking. These calculations are conducted by inserting the moment of inertia into equation 13. In order to gain some understanding of the difference between the characteristic value and the design values both values are shown here but primarily the characteristic values will be used.

Table 3.1: The values for the moment of inertia calculated from different situations.

	Moment of inertia (m^4)	Maximum load using characteristic values. (kN)	Maximum theoretical load calculated with design values. (kN)
Considering the entire cross-section	$5,589 \cdot 10^{-5}$	43,2	27,7
Gamma method	$4,87 \cdot 10^{-5}$	37,7	24,1
Assuming gamma value 0 – for example the adhesive layer completely fails – unrealistic but interesting as a reference value	$0,414 \cdot 10^{-5}$	2,99	1,9

In the rest of this thesis the moment of inertia calculated with the gamma method will be used.

3.2.5 Bending stiffness

The bending stiffness will then be calculated by multiplying the moment of inertia with the modulus of elasticity. The theoretical value will be calculated according to this method. The theoretical value uses the mean modulus of elasticity which should give a slightly lower strength than the slab has. In order to improve the accuracy of the bending stiffness it will also be calculated directly from the results of the measurement systems; this will be termed the calibrated value. These calculations will be conducted for the pairs of measurement systems along the slab. One value for strain gauge 1 and 2, one for strain gauge 3 and 4 and finally one for potentiometers 1 and 2. To calculate the bending stiffness from the results from the strain gauges (equations 2), the equation for the moment for the first load cases, were entered into equation 15, which was the equation for the moment based on strain. To calculate the bending stiffness from the results from the potentiometers the same method will be used but by for example rewriting equation 1, the equation for the deformation for load case 1.

$$M_y = \frac{E \cdot \varepsilon \cdot I_y}{y} = \frac{PL}{4} \rightarrow EI = \frac{PL \cdot y}{4 \cdot \varepsilon} \quad (24)$$

3.3 Execution of the tests

A few different test situations using static loading were tested. The sensors on the slab detected the deflection and strain. These measured values will later be used to calculate the load according to the structural codes to compare with the real load.

3.3.1 Test 1: Hydraulic actuator

Test 1 was conducted to determine the elastic properties of the slab (i.e., the bending stiffness). This can be estimated by placing weights on the slab. By gradually loading the slab with the help of a hydraulic actuator from MTS with a deformation-controlled system the entire curve can be captured. The test will be conducted three times with different loads in order to achieve as accurate results as possible.

The maximum load for the slab will be calculated for test 1 according to the characteristic bending strength. This value will be slightly lower than expected about 30-50% lower as mentioned previously in chapter 3.1.1. Since this load is only used as a reference value to check the linearity of the slab it is acceptable if the load is slightly too load. Test 1 is conducted in order to check the linearity of the slab therefore it only needs to be checked up to the level that it will be loaded with in the rest of the tests, which it is.

To create an even load on the slab, a steel beam with a width of 20 cm was placed underneath the hydraulic actuators piston as shown in figure 3.10. The test consisted of three load situations. The first load situation consisted of gradually loading the slab with a load of 1 kN/s to a maximum load of 12 kN. In the second load situation the slab was loaded with a speed of 0,1 mm/s to a maximum load of 20 kN. The first load situation was accidentally tested with

load-controlled loading, but the rest used deformation-controlled loading. Using deformation-controlled loading is a safer test method since the hydraulic actuator will then stop at the specific deflection, whereas with force-controlled loading there is a risk that the hydraulic actuator continues downwards. The force-controlled approach is also unable to capture the softening part of the curve (i.e., when the slope becomes negative). In the third load situation the slab was loaded with the same speed of 0,1 mm/s up to a maximum load of 30 kN.

For the roller bearings to function properly they must be unscrewed. The screws were forgotten in load situation 1 and 2 but removed during the third load situation.



Figure 3.10: Image of the test set up.

3.3.2 Test 2: Beam dead-loads

Test 2 consisted of using steel beams as dead loads on the slab to create different load situations. These situations are conducted in the same test after each other. The steel beams used in the test could be examples of furniture being placed in different places on the slab. The test set up is shown in figure 3.11 and the placement of the beams in the different situations is depicted in figure 3.12.

Load situation 1 consisted of beam one being placed near the strain gauge closest to the support.

Load situation 2 consisted of placing beam two on top of beam one.

Load situation 3 consisted of placing beam two closer to the middle of the slab with beam one still in its first placement.

Load situation 4 consisted of again placing on top of each other but closer to the center of the slab.

Load situations 5-8 are the same as 1-4 but on the other side of the slab, further away from strain gauges 3 and 4.

Load situation 9 consisted of placing both beams on either side of the middle of the slab.

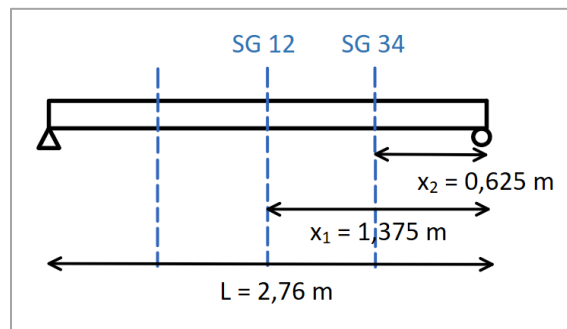


Figure 3.12: The test set up for test 2

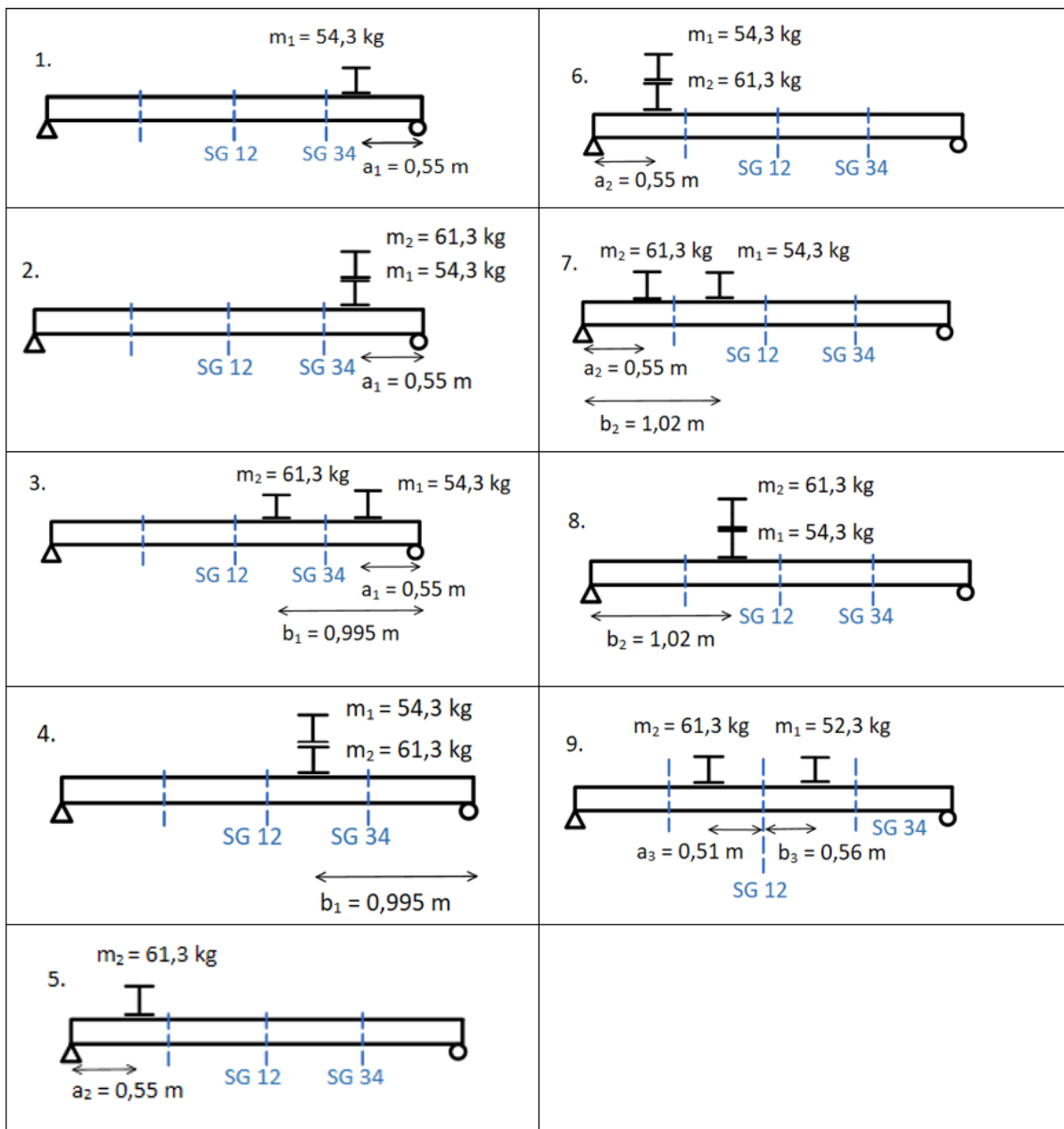


Figure 3.11: Description of the load situations.

3.3.3 Test 3: Load from people

The goal of test three is to estimate the loads from people walking on the CLT slab. To achieve this, different amounts of people walked across the slab and loaded it in different ways. Nine different load situations were tested and are described below and are also depicted in figure B.4 in appendix B.

Load situation 1 consists of two people walking across the slab.

Load situation 2 consists of two other people walking across the slab.

Load situation 3 consists of four people walking across the slab.

Load situation 4 consists of six people walking across the slab.

Load situation 5 consists of four people walking onto the slab, two people from each side of the slab.

Load situation 6 consists of two people walking onto the slab, one person from each side of the slab upon meeting in the middle they jump and then walk off the slab.

Load situation 7 consists of four people walking onto the slab, two people from each side of the slab upon meeting in the middle they jump and then walk off the slab.

Load situation 8 was prepared by placing two steel beams that represent the loads from furniture such as benches. Once the beams were placed four people walked onto the slab, two people from each side of the slab sit down on the respective beams, stand up again and then walked off.

Load situation 9 was conducted in a similar manner to test 8 but with four people, two people from each side.

Load situation 10 was prepared by placing the two steel beams along one side of the slab representing the load from a bookcase. Once the beams were placed four people walked onto the slab, two people from each side met in the middle and then walked off.

Load situation 11 consists of eight people walking across the slab.

The test people's weights and the group sizes are shown in table 3.2.

Table 3.2: Description of the groups load.

<i>Load situation</i>	<i>Amount of people</i>	<i>total load (kg)</i>
1	2	1158
2	2	1736
3	4	2766
4	6	4287
5	4	2747
6	2	1540
7	4	2865
8	2	2488
9	4	4214
10	4	3812
11	8	6893

3.3.4 Test 4: Unknown load

A test with unknown loads was also conducted to replicate a real situation. In a real situation the loads and their positions are entirely unknown, this test will investigate if these loads can be calculated. The unknown test results will be used to calculate the load based on the assumption that the load is either a point load or an evenly distributed load. Once the calculations are complete the real values will be disclosed and compared to the calculated values. A comparison between the calculated values and the real loads will follow in the discussion.

3.3.5 Test 5: Test to failure

The final test consisted of testing the slab to failure to find the maximum load that the slab could withstand. The slab was tested by using the hydraulic actuator with a deformation-controlled system using a speed of 1 mm/s. The potentiometers were removed once the slab reached 30 kN to avoid destroying the potentiometers when the slab failed.

4 Results and discussion

The results will primarily be shown in diagrams plotted against the time to show the results in a chronological order. This creates an easy comparison of the different load situations in each test. A few diagrams will also be shown depicting the load plotted against the deformation in order to confirm the linear behavior of the slab up to a certain load. All the measurement results were tared either before the start of the test or by subtracting any strain or displacement that was shown at the beginning of the test from the rest of the results.

4.1 Test 1: Hydraulic actuator

The result for load situation 3 where the slab was loaded to 30 kN is presented. Load situations 1 and 2 will not be presented since they were conducted as tests and also resulted in linear results but for lower loads. Therefore, by only presenting the linear result from the largest load in load situation 3 it can be concluded that the reaction was linear for the lower loads as well. The linear deformation can be seen in figure 4.1. The strain measured by the strain gauges was also linear as seen in figure 4.2 and followed a nearly identical pattern to the potentiometers. The trend line was linear both when the slab was loaded and during unloading. This linearity shows that the slab was in a linear elastic state during the entire duration. This proves that the slab had elastic properties up to a load of at least 30 kN.

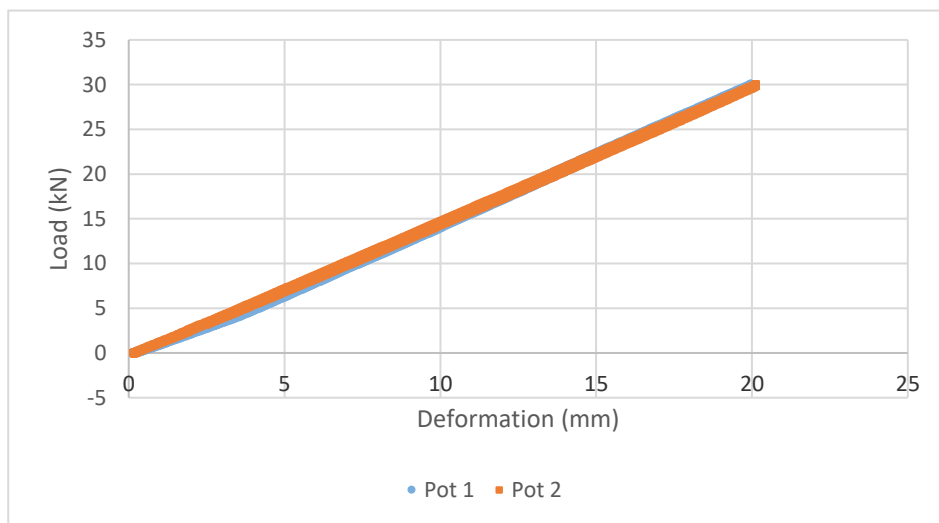


Figure 4.1: Load plotted against the deformation.

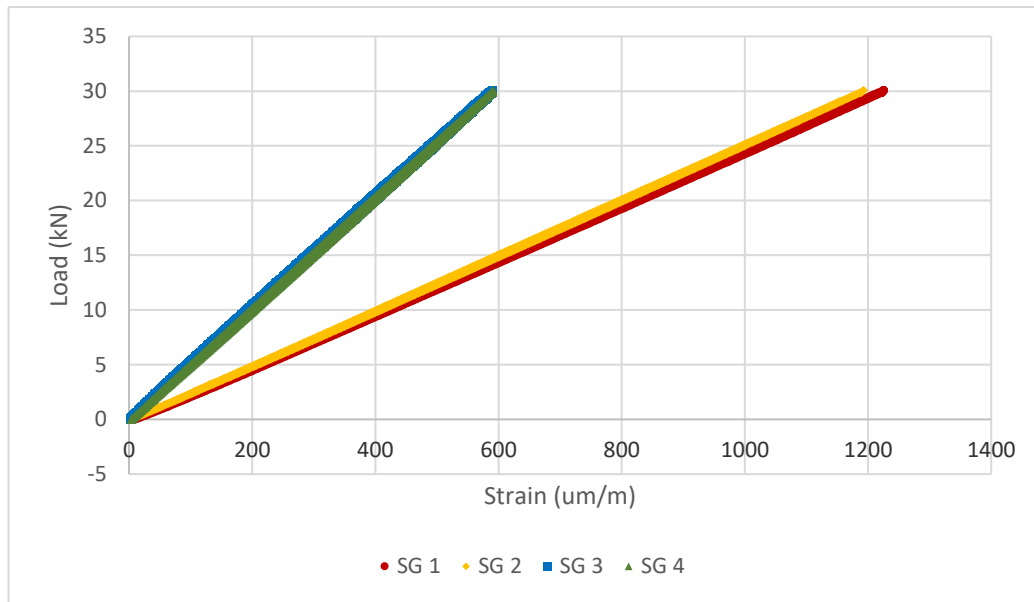


Figure 4.2: Load plotted against the strain.

4.2 Test 2: Dead-weight loading

Nine loading situations were carried out consecutively in test 2, see figure 4.3. Strain gauge 3 and 4 which were placed at the centre of the slab have a maximum strain of nearly $45 \mu\text{m/m}$ reached during load situation 2 where the two beams were placed near the middle on the side without strain gauges. Strain gauges 1 and 2 reached a maximum of roughly $35 \mu\text{m/m}$ in part 9. In part 2 two beams were placed near strain gauges 3 and 4 leading to the larger strain there. In part 9 the two beams were placed at equal distances from the middle. It is somewhat interesting to note that strain gauges 3 and 4 (quarter point) measured similar strains for part 8 and 9 even though strain gauges 1 and 2 measured different values. It is an example of how different loads can result in the same measurements and a reason for using multiple strain gauges in different locations. An interesting aspect to inspect further would be to calculate the moment at these points. Influence lines could be used to clearly depict how the moment becomes the same despite different placements of the loads.

In general, some differences can be seen between strain gauges 1 and 2. It is possible that the slab was not loaded exactly perpendicular to the beam leading to an eccentric load and therefore also an eccentric deformation. Other reasons for the measured differences are an uneven stiffness distribution in the transverse direction of the slab or the influence of local defects such as knots or unevenly placed supports. This will not be calculated further but it is an interesting point to discuss.

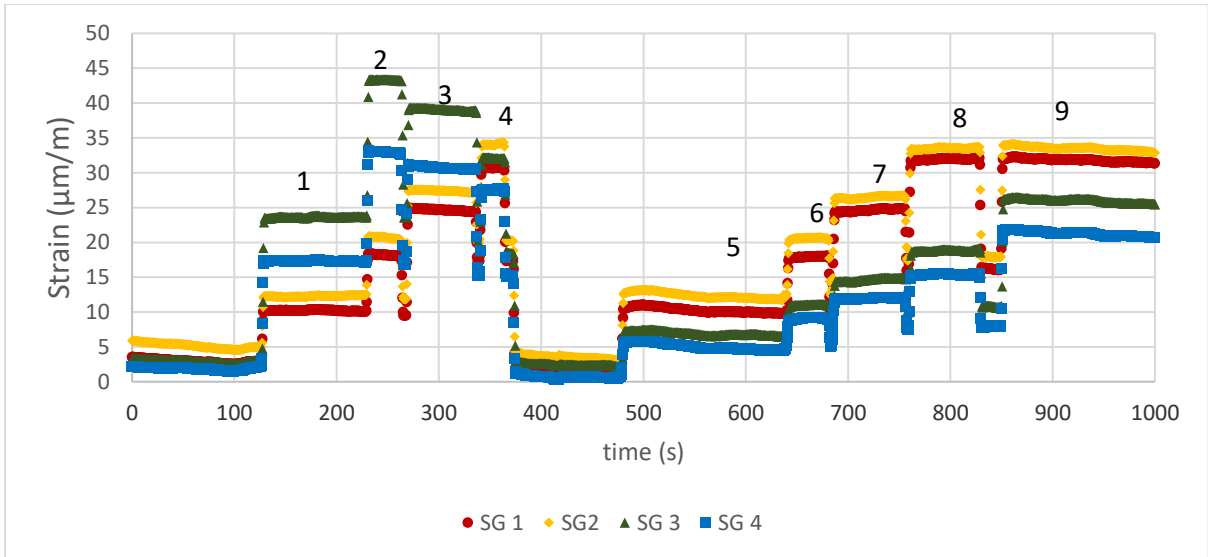


Figure 4.3: The strain results from test 2 plotted against the time.

The strain gauge has a higher precision compared to the potentiometer. On average the potentiometer seems to have measured reasonable results in comparison to the real loads which are stated in appendix 2. The results for the potentiometers can be seen in figure 4.4. At load situation 1-3 potentiometer 1 seems to be slightly lower than potentiometer 2. At load situation 8 the results for potentiometer 2 are also significantly different to potentiometer 1's results. Not only is there a difference between the potentiometers but also between the potentiometers and strain gauges 1 and 2. Since potentiometer 2's results correlate with the results from strain gauge 1 and 2 it is most likely that the error is in potentiometer 1.

The sources of error that are relevant for the strain gauge are also relevant for the potentiometer except perhaps that due to the potentiometers larger size the knots will not have as much impact. The potentiometers have a lower precision than strain gauges, which may lead to the potentiometer's values being different. Another reason for this difference may be due to the deformations being measured are quite small leading to proportionately large errors. The difference between the potentiometers could be minimized by plotting the average result of the potentiometers.

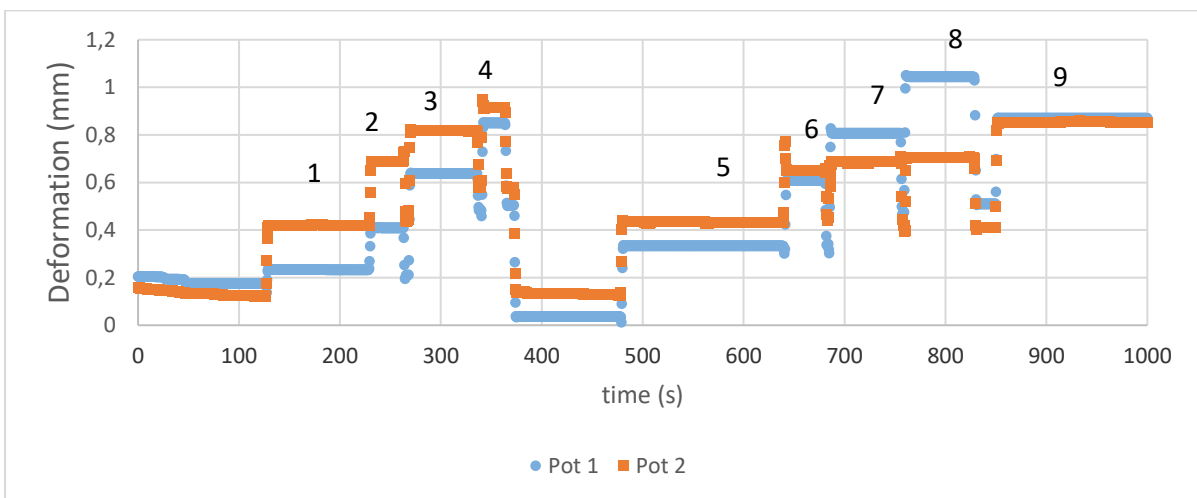


Figure 4.4: The deformation results from test 2 plotted against the time.

4.3 Test 3: Load from people

Test three consisted of allowing different groups of people to walk across the slab and conduct different activities to emulate occupancy by people. Two of the activities (load situation 6 and 7) included people jumping at the middle of the slab. This load seemed rather hard to detect by the measurement systems, this could also be due to the measuring frequency being too low.

The test results plotted against the time for the strain gauges and the deformation are seen in figure 4.5 and 4.6 respectively. The loads all peak when the people have reached the middle of the slab. As mentioned in the method for test 3 there is also an eccentric load present at load situation 10. Two beams were placed along one side of the slab, which can clearly be seen in the deformation since potentiometer 2 measures a distinctively higher deformation as soon as the beams are in place. It is interesting to note that the eccentricity nearly entirely disappears when people walk on the slab. The reason for this is that the beams weigh about the same as a small person and when a person walks on the other side the weights even out to a large extent.

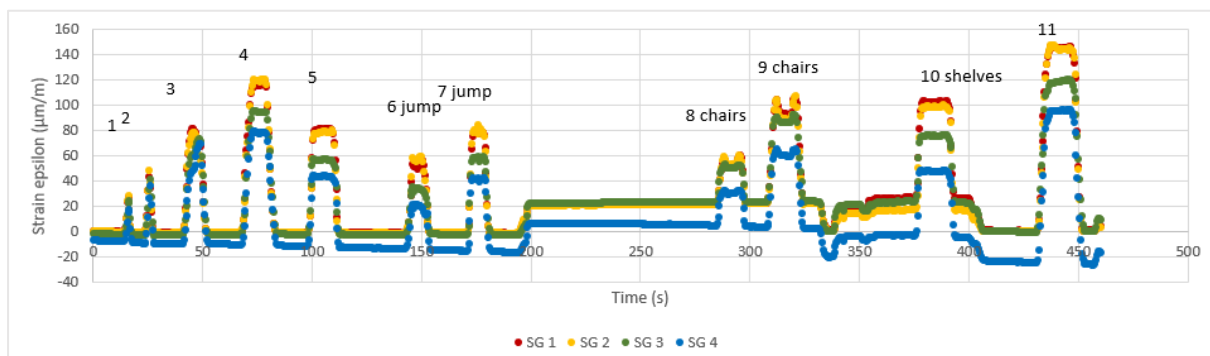


Figure 4.5: The strain results from test 3 plotted against the time.

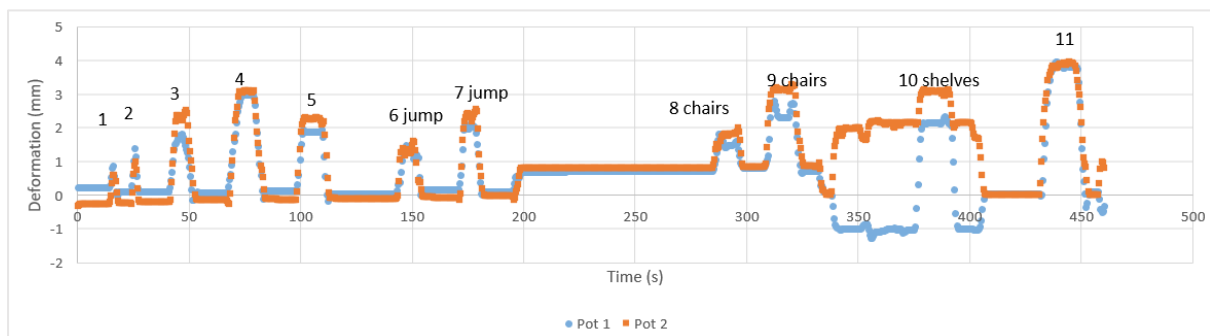


Figure 4.6: The deformation results from test 3 plotted against the time.

4.4 Test 4: Unknown load

The fourth test was conducted by the supervisor of this thesis, Ivar Björnsson. Without revealing the loads, the test results were then analysed. This test was conducted to replicate a real situation where a slab in a building could be equipped with a measuring system and used to collect data. By analysing the results, a description of the loading may be surmised. The results from the strain gauges plotted against the time are shown in figure 4.7. By analysing the data, it could be concluded that strain gauge 3 gave very different results to the other three

strain gauges. The strain had a completely different order of magnitude. The conclusion to be drawn from this is that there was some sort of error in strain gauge 3. These errors could be from simply connecting the wrong instrument to the output data or more complex such as an error with the strain gauge itself. The results from strain gauge 3 will therefore be disregarded in further analyses. It is also possible that strain gauge 4 malfunctions slightly towards the end of the test due to the measured result becoming negative, but its overall results are deemed sufficient.

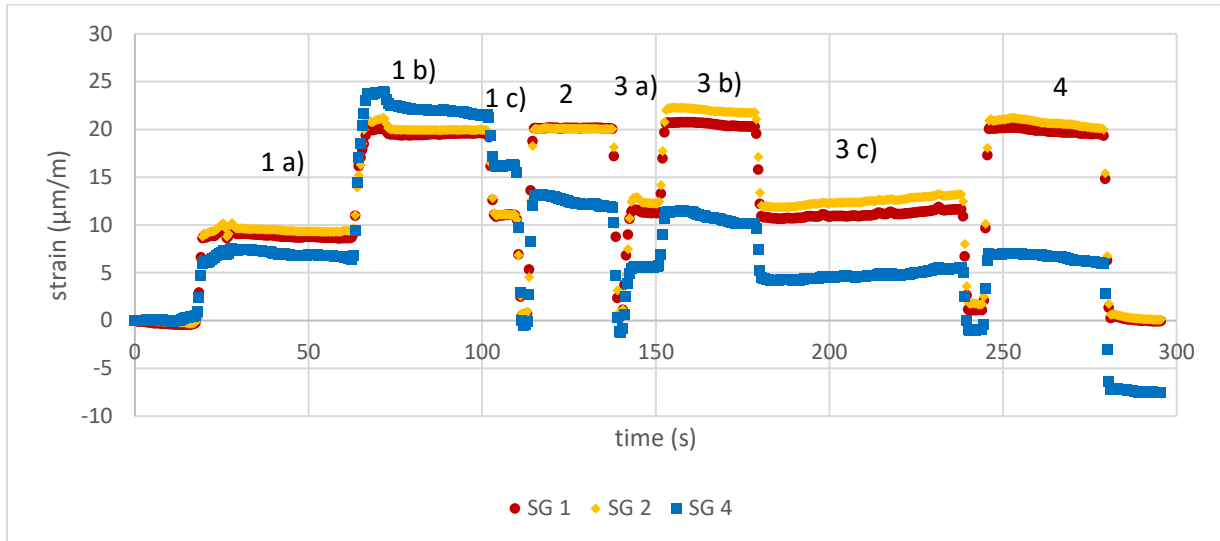


Figure 4.7: Test results from strain gauges 1, 2 and 4 for test 4

The results from the potentiometers as discussed previously were slightly less accurate than the strain gauges. The results from the potentiometers can be seen in figure 4.8. Due to the potentiometer's lower accuracy, the main hypothesis was based on the strain gauges. One aspect that is somewhat noteworthy was that the potentiometers did not show the same deformation. Since the potentiometers were on either side of the slab and showed different results, an unevenness in the slab or the load on the slab could have been expected. The strain gauges, however, did not show the same type of uneven loading in the width direction, so it was somewhat unlikely that the load was uneven and more likely that the potentiometer had an error. It seems most likely that the error is in potentiometer 1 since it has erratic behaviour below zero which is an unusual result.

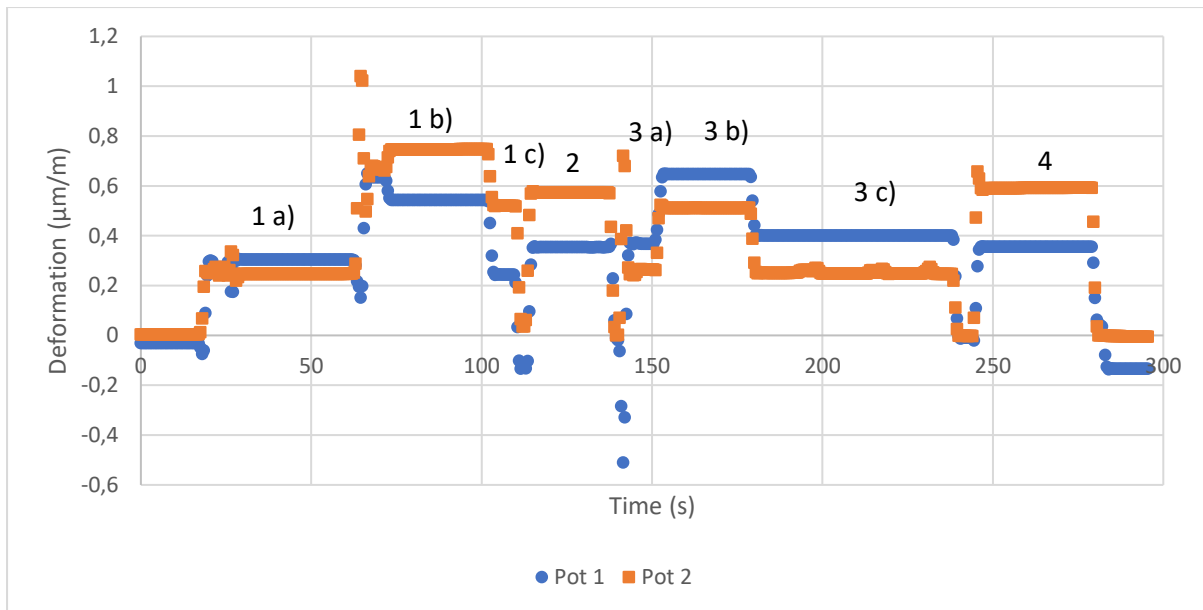


Figure 4.8: Test results from potentiometers 1 and 2 for test 3

The following results were based on an analyses of the results from strain gauges 1, 2 and 4. A timeline and description of the different events that may have occurred were hypothesised based on these results.

1. a) A load was placed on the slab. Presumably close to strain gauge 4 due to the strain being quite similar in all the strain gauges.
1. b) Another load was placed in roughly the same spot. There was a slightly larger peak at the beginning perhaps caused by impact.
1. c) A part of the load was removed
 - The entire load was removed
2. A load was placed on the slab again probably close to the middle of the slab due to strain gauge 1 and 2 showing a higher value than strain gauge 3 and 4.
 - The entire load was removed.
3. a) A load was placed on the slab on the side without the strain gauges.
3. b) A second load was placed on the slab.
3. c) The second load was removed
 - The entire load was removed
4. A large load was placed on the slab even further to the left, near the quarter point
 - The slab was unloaded.

Having made these hypotheses a general statement can also be made. The results from strain gauge 1 and 2 for load situation 1b, 2, 3b and 4 were all the same. The only difference was the results from strain gauge 4. A conclusion that can be drawn from this is the importance of a measurement system at the quarter point, without which ascertaining the actual location of the load can be quite challenging if not impossible.

4.4.1 Real load situation revealed

Once all calculations had been completed and a hypothesized result for the load cases was conducted the real load cases were revealed and compared to the hypothesized load situations. The load cases are shown in figure 4.9. The real load cases seem to correlate quite well with the hypothesized results in chapter 4.4. Case 1 in the figure correlates with the hypothesized load situation 1 b). Case 2 correlates with situation 2, case 3 correlates with situation 3 b) and case 4 correlates with situation 4.

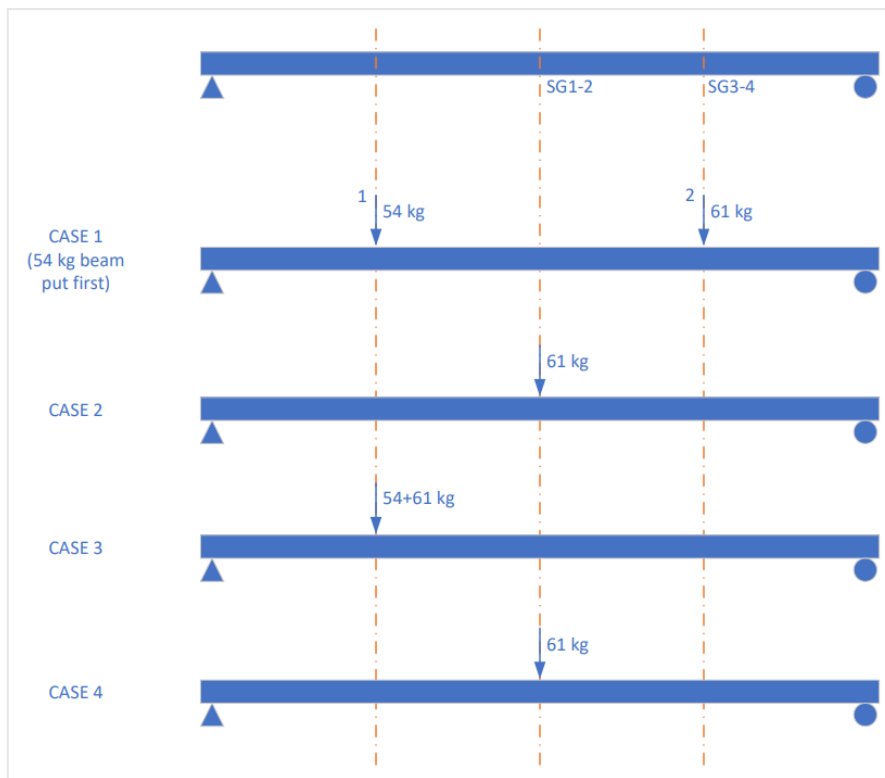


Figure 4.9: Depiction of the real load cases for test 4.

In case 1 the first beam to be placed was the 54 kg beam to the left of the strain gauges according to figure 4.9. This placement is quite similar to that of case 3 and therefore a similar reaction would have been expected. When analyzing figure 4.7 the load situation 1 a) (the first beam being placed) does not quite correlate with the results of load situation 3 a), b) and c) which has a similar load situation with the beam being placed to the left of the strain gauges. A reason for this may be that something happened to strain gauge 4 and therefore its results are significantly lower at the end of the measurement time.

4.5 Test 5: Test to failure

The aim for test 5 was to determine the actual load carrying capacity of the slab, in order to compare it to the calculated value. It is also conducted in order find any potential non-linearities at higher loads than were determined in test 1. The results from the strain plotted against the time are shown in figure 4.10. It is interesting to note that some of the strain gauges seemed to have failed before the maximum load was reached. For example, strain gauge 3 seems to have failed at a load of around 80 kN and strain gauge 1 seemed to fail at around 75 kN. The strain

gauge used in this study has a capacity of two percent according to chapter 2.4.2.2 and the maximum strain reached here was 4000 $\mu\text{m}/\text{m}$ which is only 0,4 percent. It is still possible that the strain gauges broke, for example by delamination at higher curvatures. Another aspect would be if the adhesion had failed. The strain gauges were still visibly in place but it is possible that the entire length of the strain gauge was no longer in contact and therefore could no longer measure.

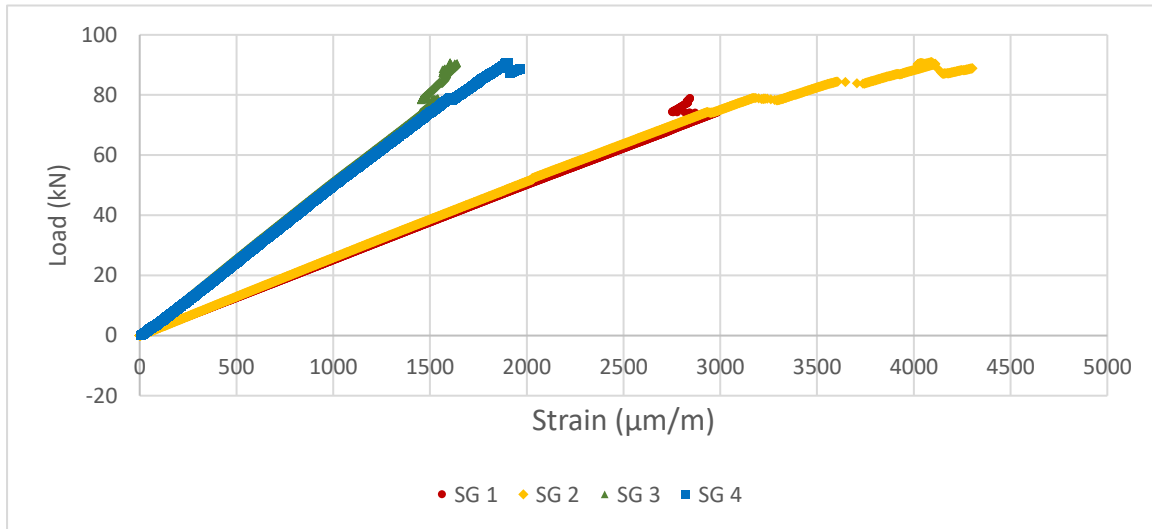


Figure 4.10: The load plotted against the strain for test 4 where the slab was tested to failure.

The results shown in figure 4.11 are from potentiometer 1, 2 and the deformation piston. The potentiometers were removed at an approximate load of 35 kN to avoid crushing them when the slab cracked. The curve for the deformation piston has some small dips, the first of which seems to occur at a load around 75 kN. These dips can be explained as small cracks occurring in the slab. The slab could still take more load and reached a maximum value a little under 90 kN.

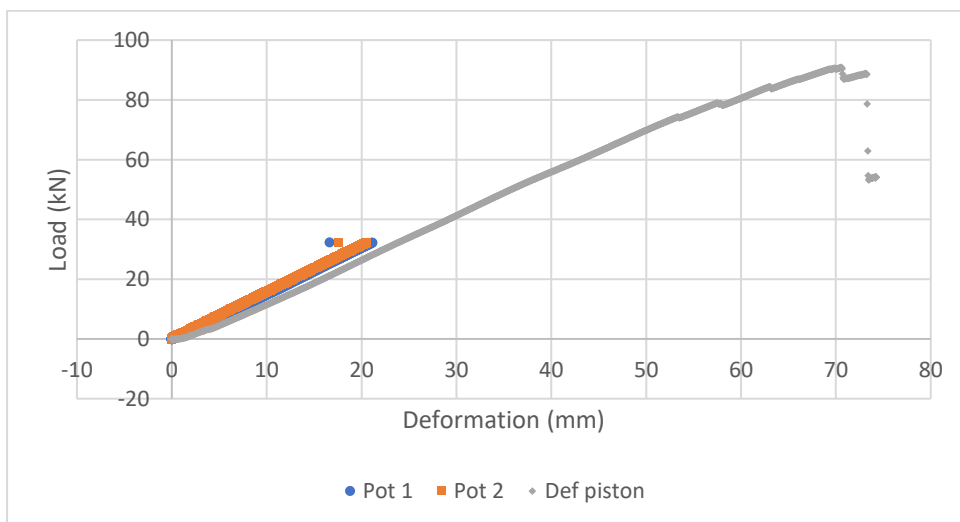


Figure 4.11: The load plotted against the deformation for test 4 where the slab was tested to failure.

The slab probably failed predominately due to ductile failure, i.e., there was a gradual loss of strength. Towards the end of the test the load was increased, and more cracks appeared. At the largest load near 90 kN a large crack appeared in the bottom layer of the CLT as can be seen in figure 4.12. The deflection of the slab can be seen in figure 4.13. It is possible that the slab had some load bearing capacity left but with a reduced cross section more loading would most likely lead to total failure and due to safety reasons, it was deemed unnecessary to load further.



Figure 4.12: Cracks in the slab at maximum load



Figure 4.13: The deflection of the slab at maximum load.

The maximum characteristic load that was calculated was 43,2 kN. This slab could be loaded with nearly 75 kN before any abnormalities occurred according to the deformation piston in figure 4.11. The slab could take a load that was more than 50 % larger than the characteristic load. This is quite reasonable since the mean value is significantly larger than the characteristic load, 30 % higher for glue laminated beams and 50 % higher for timber beams as stated in chapter 3.1.1.

5 Calculations

The calculations consist of the measurement results being used to calculate the load on the slab. The equations used for the calculations were presented in chapter 3.2.

5.1 Test 1: Hydraulic actuator

The results from test 1 were used to calculate a value for the bending stiffness according to chapter 3.2.5 to find more exact results. The bending stiffness was calculated for all the results from test 1 shown in appendix C table C.1. An average bending stiffness was then calculated for potentiometer 1 and 2, strain gauge 1 and 2 and strain gauge 3 and 4 respectively. The three different bending stiffnesses shown in table 5 below were used to calculate the load for the respective sensors.

Table 5.1: The three different values for the bending stiffness depending on the measurement system and the theoretical value.

Measurement system	Calibrated value Pot 1 2	Calibrated value SG 1 2	Calibrated value SG 3 4	Theoretical value
Bending stiffness (Nm)	$6,48 \cdot 10^{-5}$	$7,71 \cdot 10^{-5}$	$7,20 \cdot 10^{-5}$	$5,36 \cdot 10^{-5}$

The first calculations were made for load situation 1 test 1. Test 1 consisted of three different load situations as described in chapter 3.3.1, the same test was conducted but with an increasing load. The test results are shown in appendix C table C.2 and were used to calculate the point load acting on the slab with two different bending stiffnesses (EI), the theoretical value and the calibrated value calculated for the respective sensors.

The loads were calculated with the help of the load cases presented previously, reformulated so as to calculate the load.

From potentiometer measurements:

$$v_{max} = \frac{PL^3}{48EI} \rightarrow P = \frac{48EIv}{L^3} \quad (25)$$

$$M = \frac{PL}{4} = \frac{E \cdot \varepsilon \cdot I_y}{y} \rightarrow P = \frac{E \cdot \varepsilon \cdot I_y \cdot 4}{y \cdot L} \quad (26)$$

From strain gauges 3 and 4:

$$M^{0-1} = \frac{Px}{2} = \frac{E \cdot \varepsilon \cdot I_y}{y} \rightarrow P = \frac{E \cdot \varepsilon \cdot I_y \cdot 2}{y \cdot x} \quad (27)$$

The calculated loads for load situations 1, 2 and 3 are presented in appendix C table C.3 and are calculated from the theoretical bending stiffness and vary in their accuracy. The potentiometer's measured loads were about 2 kN away from the real load. The strain gauges were all about 4 kN away from the actual load, where the load results for strain gauges 1 and

2 were slightly further away from the actual load. The strain gauges only account for the local response which is due to their small size and they are also based on uniform strain. The strain in the slab is not always uniform because the strains in the timber can vary locally due to knots and cracks. To minimize this uncertainty and measure the average strain it is therefore important to use multiple strain gauges. In comparison the potentiometer reflects the entire system to a larger extent. Another method used to find a value closer to the actual load was to use the calibrated bending stiffness. These calculations resulted in a higher accuracy which can be seen in figure 5.1.

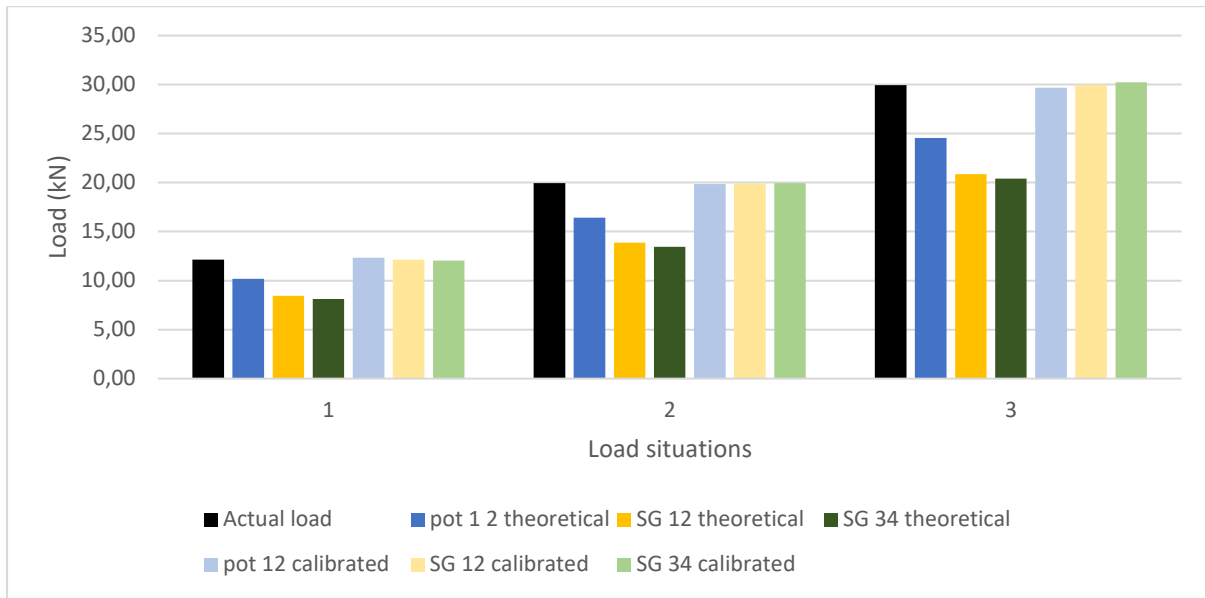


Figure 5.1: Test 1: The actual load compared to the calculated loads.

By calculating the difference between the calculated loads and the real load a percentage of the error can be found. These values are shown in figure 5.2, clearly depicting that the calibrated values have a percentage of error that is near zero whereas calculations using the theoretical value for the bending stiffness has an average percentage of error that is nearly 27%. The deformation piston was not used to calibrate the load due to it having a higher uncertainty than the other measurement systems.

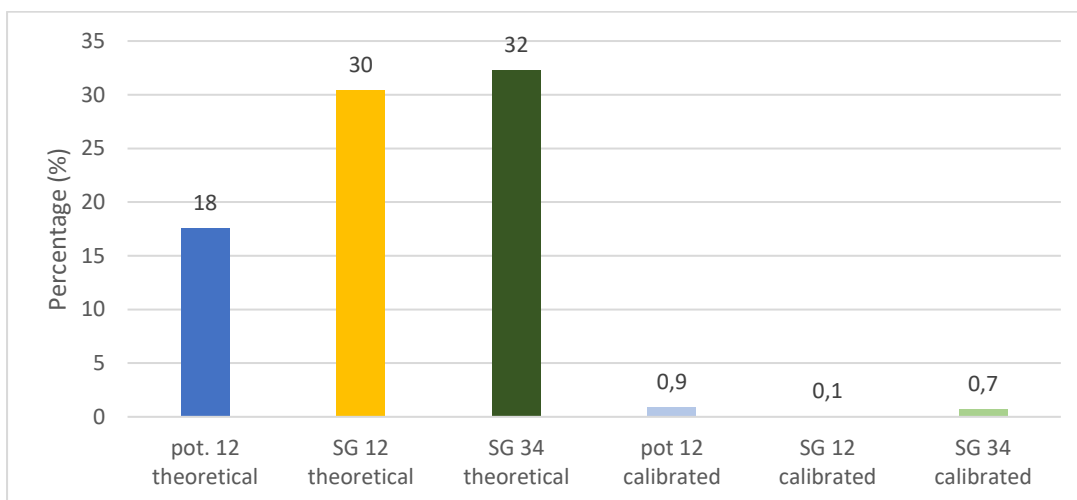


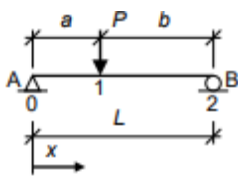
Figure 5.2: Test 1: Percentage of error for the calculated point load compared to the real load.

5.2 Test 2: Dead-weight loading

Test 2 consisted of a non central load. The load was calculated from the deformation as shown in equation 28.

$$v_{mitt} = \frac{Pa(3L^2 - 4a^2)}{48EI} \rightarrow P = \frac{v_{mid} \cdot 48 \cdot E \cdot I}{a(3L^2 - 4a^2)} \quad (28)$$

The load was also calculated from the strain. The values for the first load situation are given in figure 5.3. The x value stands for the distance to the strain gauges and is shown in figure 3.11, where x_1 is used for strain gauges 3 and 4 and x_2 for strain gauges 1 and 2.



$$M^{0-1} = \frac{E \cdot \varepsilon \cdot I_y}{y} = \frac{Pbx}{L} \rightarrow P = \frac{E \cdot \varepsilon \cdot I_y \cdot L}{y \cdot bx} \quad (29)$$

$$M^{1-2} = \frac{E \cdot \varepsilon \cdot I_y}{y} = \frac{Pa(L-x)}{L} \rightarrow P = \frac{M \cdot L}{a(L-x)} = \frac{E \cdot \varepsilon \cdot I_y \cdot L}{y \cdot a(L-x)} \quad (30)$$

Figure 5.3: Load case 2

These calculations take into account the fact that the load is not placed centrally and are only made for load situations 1, 2, 4, 5, 6 and 8. The results for the calculated noncentral loads for test 2 are shown in appendix D table D.2 and can also be seen in figure 5.4.

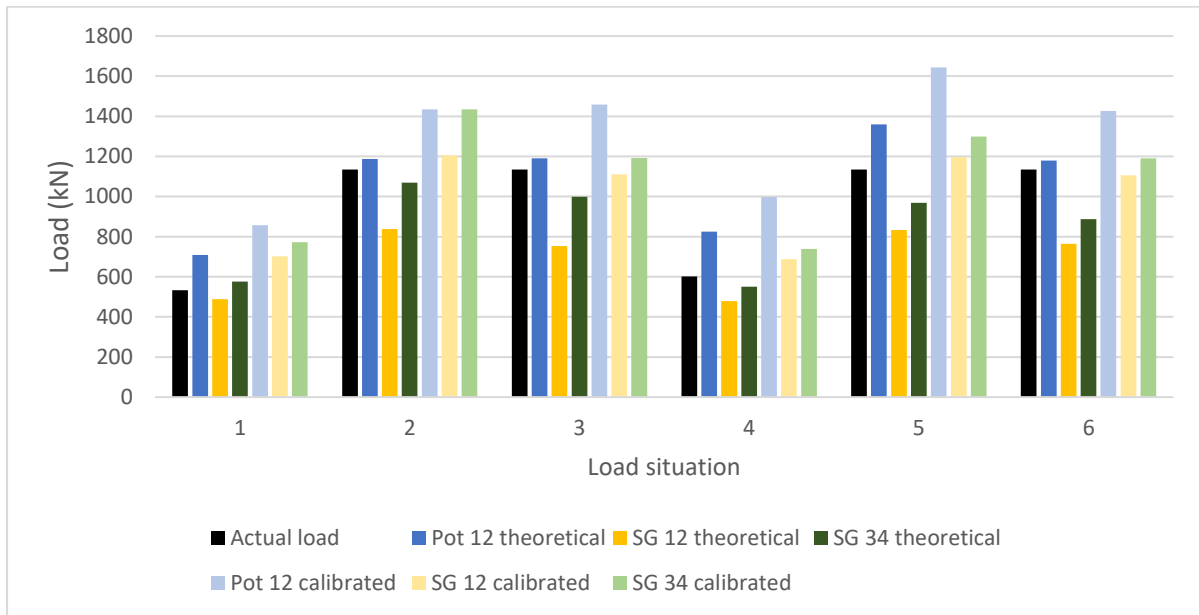


Figure 5.4: A comparison of the load calculated with consideration to its placement and the actual load for test 2.

In table 5.2 below the results for load situations 1 and 2 show that at the middle of the slab on the side with pot 2, and SG2 the loads seem to be slightly larger. At the quarter point of the slab the side with SG 3 seems to be loaded slightly more than the other. This could be due to an unevenness of the placed load or structural unevenness within the slab. It is also worth noting that the sensors are placed at different distances from the middle of the slab. Another aspect is that the load itself is quite small and the measurement accuracy becomes quite important. In reference to load situation 2 the strain at the quarter point is larger than the midpoint. This is

due to the noncentral load leading to a larger strain at the quarter point than in the middle of the slab.

Table 5.2: The calculated noncentral point

Load situation	Load (N)	Calculated with bending stiffness (EI):	Central point load (N) calculated from the respective measurement systems					
			Def1	Def2	SG 1	SG 2	SG 3	SG 4
1	533	Theoretical	504	912	446	531	665	486
		Calibrated	610	1103	641	763	892	652
2	1134	Theoretical	885	1488	785	892	1215	923
		Calibrated	1070	1800	1128	1282	1630	1238

The second calculation will include all the load situations and will calculate the uniformly distributed load and a central point load. The uniformly distributed load can be compared to the value for the imposed load. The calculations for the imposed load are shown in equations 31-33.

$$v_{max} = \frac{5qL^4}{384EI} \rightarrow q = \frac{v_{max}384EI}{5L^4} \quad (31)$$

$$M_{max} = \frac{qL^2}{8} = \frac{E \cdot \varepsilon \cdot I_y}{y} \rightarrow q = \frac{8 \cdot E \cdot \varepsilon \cdot I_y}{y \cdot L^2} \quad (32)$$

$$M = \frac{qLx}{2} - \frac{qx^2}{2} = q \left(\frac{Lx - x^2}{2} \right) = \frac{E \cdot \varepsilon \cdot I_y}{y} \rightarrow q = \frac{2 \cdot E \cdot \varepsilon \cdot I_y}{y \cdot (Lx - x^2)} \quad (33)$$

Imposed loads are generally uniformly distributed, they do not account for how the actual load varies along the slab. The reason why imposed loads are still used is that it is important to have a model which is sufficiently simple to be used in practice. Point loads are used in some cases but primarily for large loads or unusual buildings and not in an office building. For use in a practical situation calculating the load for the middle of the beam is slightly simpler, which can be advantageous when calculating dimensions because it saves time. The uniformly distributed load and the point loads are calculated and shown in table D.3 in appendix D. These calculations do not give the actual value of the load but instead give an idea of how these loads compare to the results for the uniformly distributed loads calculated in test 3 and 4 and can also be compared to the value for the uniformly distributed imposed load.

The central point loads for test 2 are shown in figure 5.5. In comparing the real noncentral loads and the calculated loads from strain gauge 1 and 2 as well as from the potentiometers, it can be observed that these correlate well. The loads calculated from strain gauge 3 and 4 on the other hand differ significantly. In the first 4 situations the load is closer to strain gauges 3 and 4 leading to a large strain there and a deceptively large load. In the same manner the load is placed further away from strain gauges 3 and 4 in the last 4 tests and therefore the results are smaller. The final load was placed in a relatively central position resulting in a more even result from all the measurement systems.

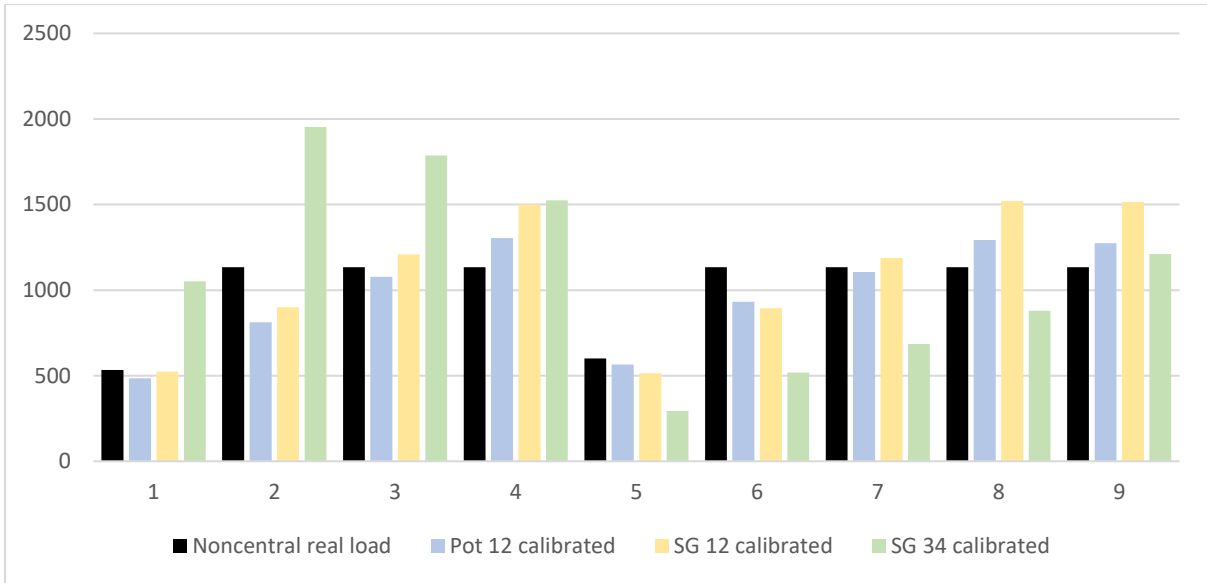


Figure 5.5: The calculated central point load not considering the actual placement of the load compared to the actual load for test 2.

The difference between the calculated load and the real load can be determined, which can be used to find the average of the difference for each measurement type. These average differences are shown in figure 5.6 below.

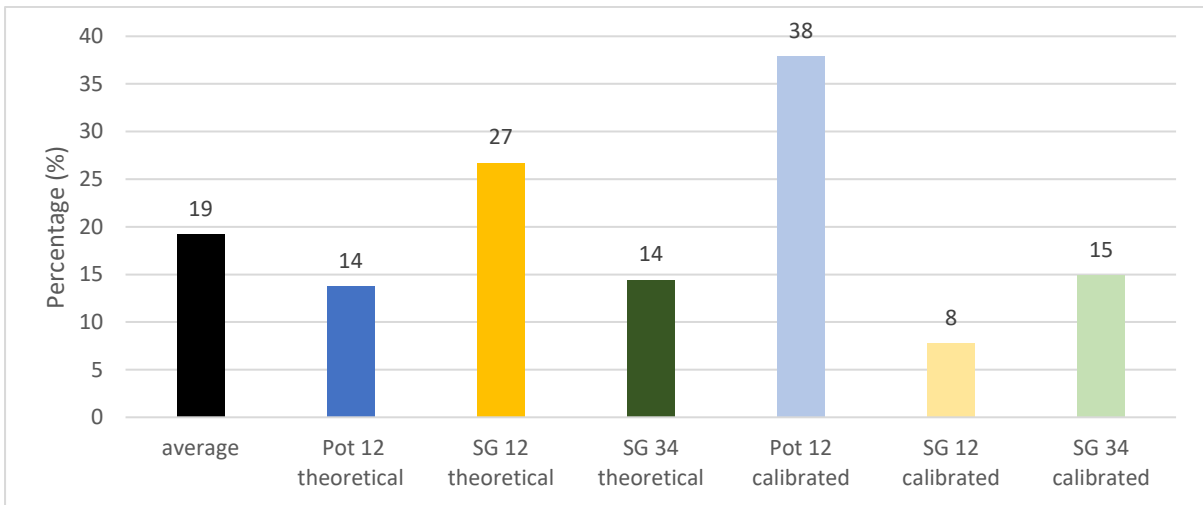


Figure 5.6: The percentage of error between the total load in comparison to the noncentral load for test 2.

According to figure 5.6 the total percentage of error was lowest for strain gauge 1 and 2 using a calibrated value for the calculations, the error was 8 %. The average error for all the measurement systems was 19 %. Unfortunately, using the calibrated values from potentiometer 1 and 2 yielded a rather large error of nearly 40 %. It is possible that the calibrated value was not as exact as expected. It is also of interest to note that these values are normal averages comparing the total difference. As in they do not take into account if the measured value is higher or lower than the actual value. The loads calculated with the theoretical value were often lower than the real loads, except for the loads calculated from the potentiometer results, where the loads were higher. When using the calibrated value, the calculated load was always larger than the actual load. A conclusion that could be drawn from this is that in a realistic situation where safety is the most imperative point it would be more important to use the calibrated value

to avoid calculating a load that is too small. The theoretical value for the bending stiffness is based on the mean value. This value would be found if multiple experiments were conducted on multiple slabs but since this experiment is limited to one slab the value may vary.

5.3 Test 3: Load from people

The calculations for test 3 are very similar to test 2 where the calculations use the load cases for a point load in the middle of a beam and a uniformly distributed load. Overall, the calculated loads match the maximum load created by the people quite well, as seen in figure 5.7 below. The measurement results and the exact load values are given in appendix E in tables E.1 and E.2 respectively. The test people’s weight was not measured on site but was an estimated weight the test people gave which could lead to some differences in the test results.

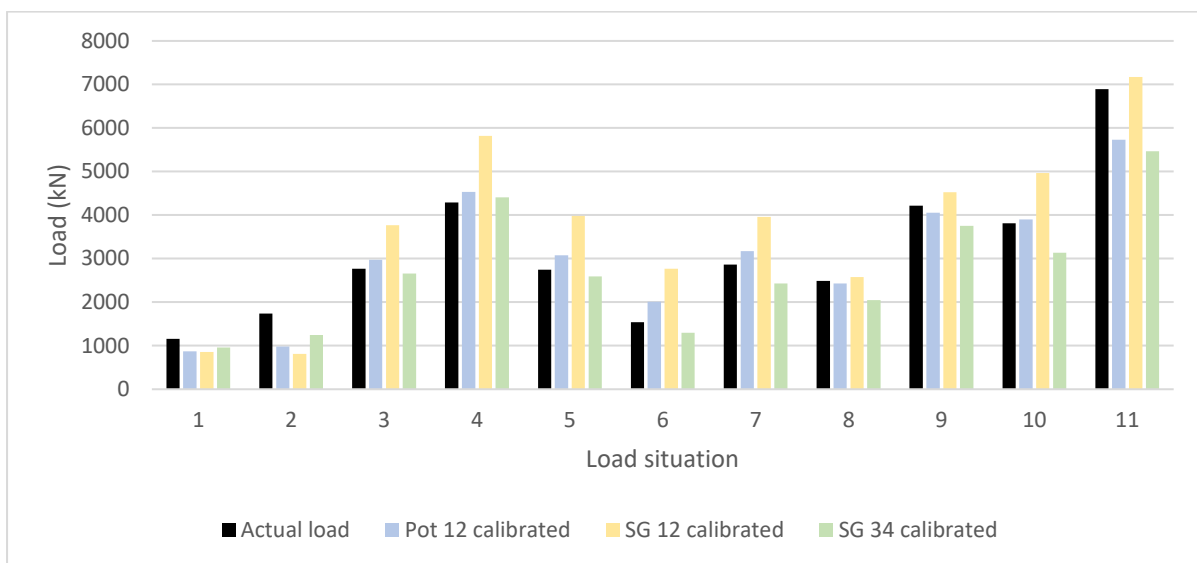


Figure 5.7: The calculated point load compared to the actual load for test 3.

The largest measured uniformly distributed load is $3,3 \text{ kN/m}^2$ and occurred when eight people were standing on the slab. This is larger than national load of $2,5 \text{ kN/m}^2$ but that is not unexpected. The amount of people on the slab can be calculated as an average of 2,7 people per square meter. Figure 2.4d shows the density of 2,5 people per square meter, it could be speculated that people don’t often stand in such proximity when in an office environment. So, it should be safe to assume that a load of $3,3 \text{ kN/m}^2$ is a load that rarely occurs solely due to human loads. Despite this, it is important to remember that furniture and equipment play a large role in the imposed load.

In figure 5.8 the percentage of error for the calculated point load is shown. The results were calculated in the same way as mentioned in test 1 and 2. The average error for this test was 14 %, in comparison to test 2 which had an average error of 20 %, the result from this test was therefore more accurate. This is most likely due to the load being centrally placed which simplifies calculations. Most of the loads calculated from the values from the potentiometer and strain gauge 1 and 2 were lower than the actual load, whereas for strain gauge 3 and 4 the values were mostly higher. As mentioned in test 2, it is better to have an over dimensioned value from a safety perspective, in that manner it may be preferable to use strain gauge 3 and 4 in order to ensure that the largest load is measured. But considering the margins of error it would be best to conduct more tests in order to state this definitively.

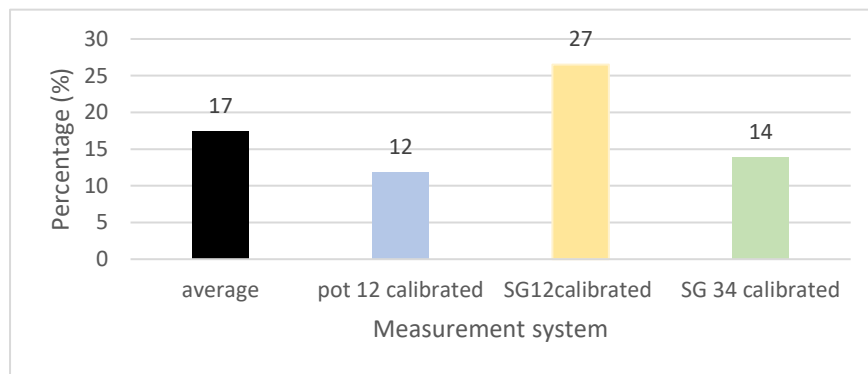


Figure 5.8: The percentage of error for the calculated point load compared to the real load for test 3.

5.4 Test 4: Unknown load

The calculations for test 4 were made with an unknown real load. Therefore, it was not possible to compare the calculated load, instead the focus in this test was on calculating a possible real load with the help of the measurements. In order to make a hypothesis on the size of the load two load cases were used in the calculations, the load case for a point load in the middle of a beam and for a uniformly distributed load. The calculations were conducted in the same manner as the previous tests. The results from the calculations are shown in figure 5.9 for the point load and 5.10 for the uniformly distributed load. The results from the calculations gave different average values, but they seem proportionately reasonable in relation to each other. The measurement results and the calculated loads can be seen in appendix F in table F.1 and F.2 respectively.

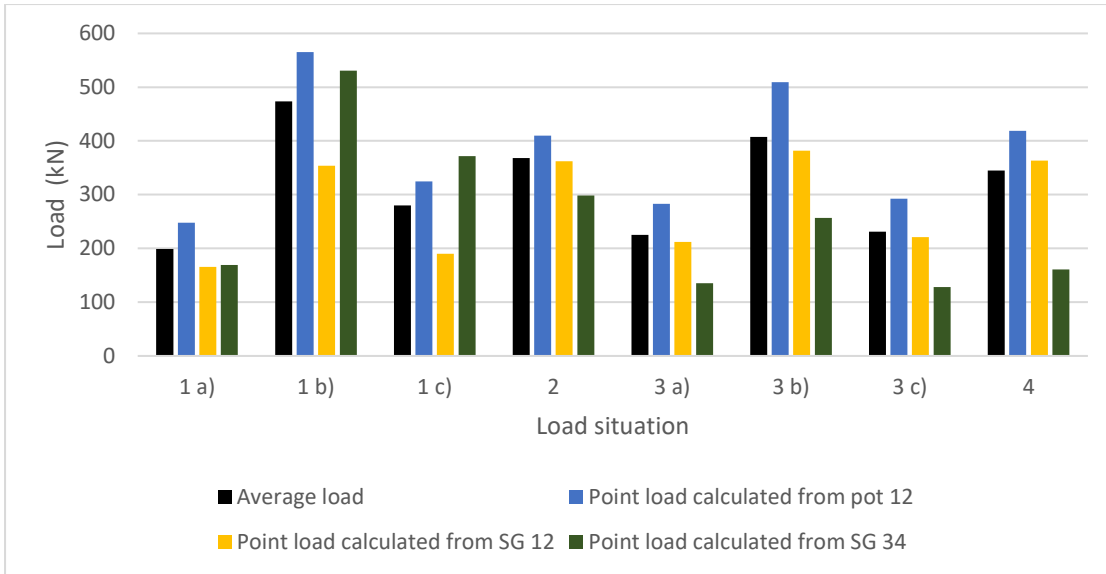


Figure 5.9: The hypothesized evenly distributed load for test 4

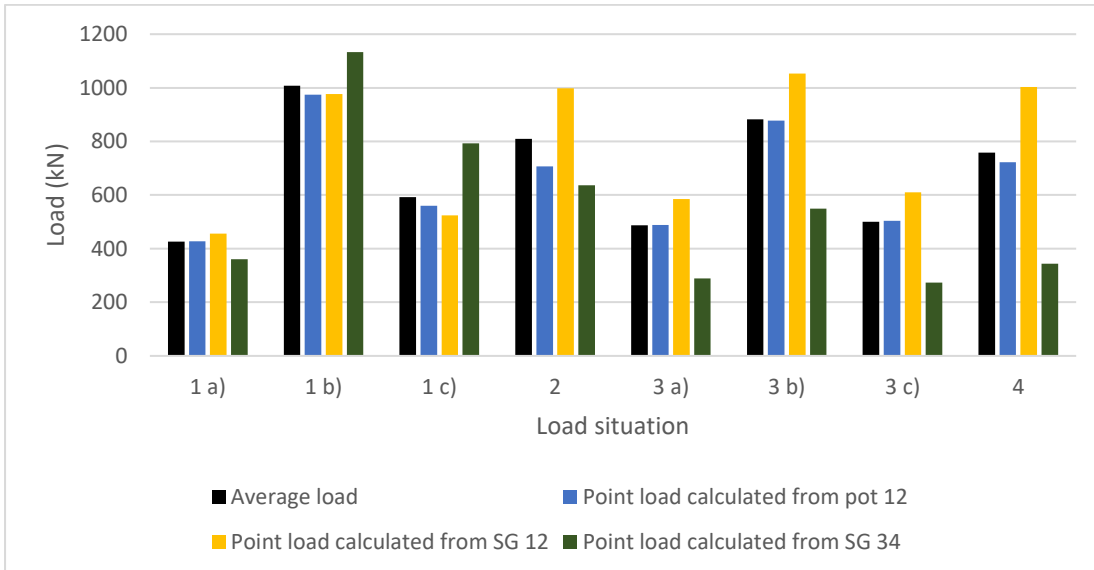
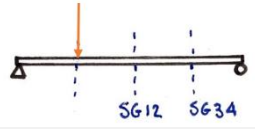
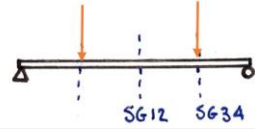
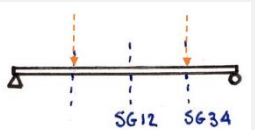
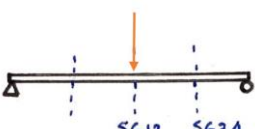
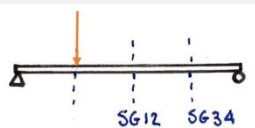
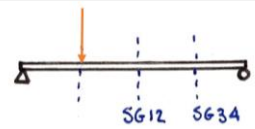
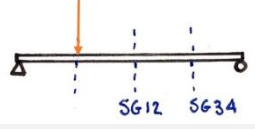
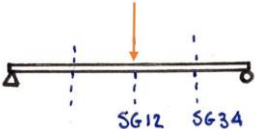


Figure 5.10: The hypothesized point load for test 4

5.4.1 Real load situation revealed

Once all calculations had been completed the real load was revealed. The loads are presented in table 5.3 according to the load situations stated in the hypothesis.

Table 5.3: The real loads compared to the hypothesized loads.

Hypothesized load situations	Position	Real load (N)	Hypothesized point load in the middle of the slab (N)
1 a)		530	419
1 b)		1128	997
1 c)		Unknown which beam was moved first. 530 or 598	590
2		598	792
3 a)		Unknown which beam was placed first. 530 or 598	476
3 b)		1128	862
3 c)		Unknown which beam was removed first. 530 or 598	488
4		598	737

From the table above one can draw the conclusion that the calculated loads are all greater than the hypothesized loads. Few of the loads are centrally placed and yet the load values are rather similar.

6 Discussion

The purpose of this study was to compare different types of sensors that could be used for measuring the imposed loads on buildings. This was achieved in part by the literature study of different measurement systems and in part with the tests using strain gauges and potentiometers.

How accurately can the load affecting a CLT slab, in a building, be calculated by using measurement data from measurement systems?

Calculating the load on a CLT slab was successfully conducted in this report and indicates that it is a possible method to use in future load measuring situations. To achieve more accurate results, a bending stiffness can be calculated with measurement results. This calibration procedure leads to more accurate load values due to the differences between standards and the actual material that is used. In a real situation the bending stiffness can be calculated but the boundary conditions must be known. Depending on the different boundary conditions different load cases are used to calculate the bending stiffness.

The results can be affected negatively by

- errors in calculations,
- incorrect strength values,
- and faults with the measurement system.

These sources of error have the potential to greatly impact the measured values and the accuracy. A calculation error could lead to the result having an incorrect order of magnitude which is a mistake that cannot be overlooked. Similarly faults with the measurement system as seen in test 4 can lead to extremely large, measured values, therefore values must be checked that they are of a realistic size.

For test 1, 2, and 3 a percentage of error was calculated. In test 1 the calibrated value gives an incredibly accurate value near zero which is due to the value being calibrated from that test. Unfortunately, the calibrated value is not quite as accurate in test 2 but is still better than the theoretical value. The average percentage of error for test 2 was 19 % and test 3 was 17 %. The most precise results from the measurement systems was 8 % found in test 2, figure 5.6 for strain gauge 1 and 2. The least accurate value was 38 % which was measured for potentiometer 1 and 2 in test 2 unfortunately this points to a large margin of error, and more tests would be needed to find more definitive results.

A difficulty with measurement systems is that each value is only valid for that specific point. To have a full understanding of the entire slab a large amount of measurement systems would have to be used. This becomes an optimization problem where the potential benefits of additional sensors would have to be compared to the costs. The reliability of sensors is also a relevant issue to consider in this problem. For example, by applying a minimum of two sensors in comparison to one sensor the risk for error decreases substantially due to the ability to compare the two values and discard unrealistic results, such as those that occurred in test 4.

How feasible is it to use different measurement systems for imposed loads?

In this report the focus was on point loads and uniformly distributed loads. This was a chosen limitation but allowed for simpler calculations, which is in line with the design procedure specified in the structural design codes (Eurocodes). Due to the standards being primarily based on distributed loads it was deemed a relevant way to compare the loads. To have an exact replica of the load situation, with each load depicted individually would of course be more precise but may also be overly complex. Due to the uncertainty of which load situations can occur, depicting the loads in the correct load situation may not make as large of an impact on the design load as expected.

In the future it may be possible that by collecting more data and information about the imposed loads a modelling system for imposed loads could be created. By simulating many different specific load situations, a new design load could be determined based on the collection of imposed load data for certain buildings. This modelling system could potentially be created with the help of modern technology and digitalization. By creating this system, it is possible that the design imposed loads used today could become more representative and potentially lead to lower loads. With lower loads smaller dimensions could be used and less material would be used.

If a smaller imposed load were found with the help of modeling systems, it may not have as great an impact as first assumed. This is due to the other requirements apart from the structural stability that must be fulfilled. For example, the acoustic requirements and the fire safety regulations.

How could a measurement system be designed in a realistic situation?

Table 6.1 presents a comparison of the different measurement systems presented in chapter 2.4.2. This is a limited study and the accuracy gradings are based on an overall understanding of the measurement systems based partly on the literature study.

Table 6.1: comparison of the measurement systems.

<i>Measurement systems</i>	<i>Measurand</i>	<i>Accuracy</i>	<i>Price</i>	<i>Reusable</i>
<i>Potentiometers</i>	Deformation	Low	\$\$	Yes
<i>Linear Variable Displacement Transducers (LVDT)</i>	Deformation	Adequate	\$\$	Yes
<i>Strain gauges</i>	Strain	Adequate	\$	No
<i>Strain transducers</i>	Strain	Good	\$	To some extent
<i>Fiber Bragg grating (FBG)</i>	Strain	High	\$\$\$	Yes
<i>Load cells</i>	Load	Good	\$\$	Yes
<i>Laser Doppler Vibrometers (LDV)</i>	Deformation	Excellent	\$\$\$	Yes

To use measurement systems in a realistic situation it would be ideal to implement them during the construction stage. One of the most fitting measurement systems would be the LDV due to its accuracy but due to its size and cost it would be difficult to implement. A strain gauge has

an appropriate size but due to its sensitivity it can very rarely be reused. A strain transducer would therefore be a good choice due to its size, protection, and slightly increased accuracy in comparison to a strain gauge. The chosen measurement system could then be placed beneath a slab and then covered with a suspended ceiling. The measurement system would not affect the finished product, either structurally or aesthetically. The suspended roof would also provide the measurement system with an extra layer of protection. On the other hand, by incorporating the measurement system in the building would become quite difficult, if not impossible to reuse. This is relevant for all the measurement systems mentioned in table 6.1 that are reusable. Therefore, using a strain gauge, which is not reusable, may not be as bad as first assumed, at least from an economic point of view.

As previously stated in this thesis the design loads are often over dimensioned. The literature study in chapter 2.1.1.3 describes the Swedish standard which states that people should have generally have a little more than one square meter per person. The British standards state a general value of 12 square meters per person for dimensioning the total area in office environments. If these values for people per square meter were calculated as loads it would be much lower than the design load of 2,5 kN/m² according to Boverket. It is of course important to include other loads from the office such as the loads from equipment and furniture. On the other hand, the load from bookshelves has likely changed over the years, with the help of digitalization less information is being stored in its physical form, such as books, therefore this load has likely become smaller over the years. An interesting comparison is the different loads that occurred from the test people. The largest load occurred with eight people on the slab. In comparison to both the Swedish and the British standards the people were standing much closer, and yet the total load isn't larger than the design load from Boverket.

Today open plan offices are becoming more and more popular. These offices may allow for more efficient use of space which could potentially lead to more people per square meter and higher loads. One of the aims of open plan offices is often to have more natural meetings between people. This may lead to more groupings of people as opposed to sitting at assigned desks which is a more evenly distributed load.

7 Conclusion

I have throughout this work shown and discussed the importance of an accurate value for the imposed load. Measurement systems are a possible solution to fulfill the need for more information on and to reach a more accurate value for the imposed load. The tests showed that a margin of error of eight percent could be reached with the use of a strain gauge in the middle of a slab, this result was for a limited test sample and requires further testing but there is great potential within these measurement systems. By implementing measurement systems in realistic situations real loads could be measured during the lifetime of a building, leading to a greater understanding of the imposed load. The test showed that it is indeed possible to implement measurement systems such as strain gauges and potentiometers to accurately measure the load that a slab is subjected to. With these findings there is the potential to minimize the imposed load and minimize the dimensions of load bearing structures which in turn may lead to a decrease in material waste. Efficient use of building material can lead to environmental and economic advantages which is precisely why this is of interest in order to improve the future of the construction sector.

8 Future studies

To improve the results from this study it would be interesting to recreate the test for more slabs, to better capture the variation due to different materials and manufacturing. Also testing different types of slabs both timber and concrete slabs could be of interest. Another opportunity for future studies would be to install measurement systems in real buildings which would allow for realistic loads to be measured. This would greatly improve the results of this test by giving a realistic image of which loads impact the slab. If realistic data was collected over a longer period, the data could potentially be used as a basis for updating the values provided in the design code. It could also be used to provide an improved basis for the probabilistic models for imposed loads.

Future studies could choose to focus on other aspects of the load for example dynamic impacts, impulsive actions, such as jumping, may not often occur in an office environment, however, having more data on how this type of activity influences the load bearing system allows for a more accurate load to be calculated. It would also be of interest to inspect the vibrations created by different loads since vibrations in wood have the potential to impact the dimensions needed significantly. Creating a study more focused on long term loads would also be of great interest due to realistic loads often lasting for long periods of time. Furthermore, certain building materials such as timber and concrete have time-dependent responses to loading. The variation of the load in space is also an interesting aspect that could be investigated, in particular the impact of eccentric loads. In this study the calculations for the slab were simplified to a simply supported beam with a flexural response, for potential future studies it could be of interest to calculate the load positions more specifically.

Another property that could be examined more closely are the boundary conditions. This study only looked at a slab bearing load in one direction, there are many slabs that bear weight in both directions. This could lead to the load behaving differently and since the slab is better supported it is possible it would require a smaller dimension. This study focused on a simply supported slab, however, in a real situation, slabs are often fully restrained due to the loads from walls and the floors above. The amount that the slab is restrained with depends on the number of floors above, the floor on the lowest level with multiple floors above will be the most fully restrained whereas the floor on the highest level may not be quite as restrained. As mentioned previously the different boundary conditions lead to different load cases and if the wrong load case is chosen it could significantly impact the accuracy of the calculated load. Therefore, this would be a relevant aspect to conduct further research on.

9 References

- Aicher S, Hirsch M and Zachary Christian (2016) Hybrid cross-laminated timber plates with beech wood cross-layers. *Construction and Building Materials* Volume 124. Available at: <https://www.sciencedirect.com.ludwig.lub.lu.se/science/article/pii/S0950061816313149?via%3Dihub> (accessed 2022-03-11).
- Al Ali M, Platko P, Bajzecerova V, et al. (2021) Monitoring the strain of beech plywood using a bistable magnetic microwire. *Sensors and Actuators A: Physical* Volume 326. Available at: <https://www.sciencedirect.com.ludwig.lub.lu.se/science/article/pii/S0924424721001898?via%3Dihub> (accessed 2022-03-11).
- Anshari B, Guan Z, Kitamori A, et al. (2012) Structural behaviour of glued laminated timber beams pre-stressed by compressed wood. *Construction and Building Materials* Volume 29. Available at: https://www.researchgate.net/publication/251621202_Structural_behaviour_of_glued_laminated_timber_beams_pre-stressed_by_compressed_wood (accessed 2022-03-11).
- Bajpai P (2018) Biermann's Handbook of Pulp and Paper (Third Edition). Volume 2: Paper and Board Making: 483-492. Available at: <https://www.sciencedirect.com/science/article/pii/B9780128142387000246> (accessed 2022-03-20).
- Bajzecerová V (2017) Bending Stiffness of CLT-Concrete Composite Members - Comparison of Simplified Calculation Methods☆. *Procedia Engineering* 190: 15-20.
- BDI (n.d.) *ST350 STRAIN TRANSDUCER*. Available at: <https://bditest.com/product/st350-strain-transducer/>. (accessed 22-02-03).
- Bengtsson E and Sandberg E (2020) *Analys av nyttig last vid dimensionering av kontorshus*. Lund University, Lund, Sweden. Available at: <https://lup.lub.lu.se/student-papers/search/publication/9013269#:~:text=I%20Sverige%20finns%20kravet%20att,a%20att%20b%C3%A4ra%2070%20personer>.
- Blaß HJ and Sandhaas C (2017) *Timber Engineering - Principles for Design*. Karlsruhe: KIT Scientific Publishing
- Boverkets (2019) Boverkets konstruktionsregler

- EKS 11. Available at:
<https://www.boverket.se/globalassets/publikationer/dokument/2019/eks-112.pdf>.
- Cardei P, Matache M, Persu C, et al. (2021) Simulation of the Calibration Process of the Strain Gauge Measurement Systems. In.: IEEE. Available at:
<https://dx.doi.org/10.1109/ecai52376.2021.9515181>. DOI:
10.1109/ecai52376.2021.9515181.
- Carlsson F, Andersson A, Enckell M, et al. (2007) Modern mät- och övervakningsmetodik för bedömning av befintliga broar. Report, KTH Stockholm: Institutionen för Bygghvetenskap.
- Chen H-P and Ni Y-Q (2018) Sensors and Sensing Technology for Structural Monitoring.
- CIB (1989) Actions on Structures - Live Loads in Buildings. Reportno. Report W81 - Publication 116.
- Elkome (2016) *ACT LVDT Displacement Transducer - Data sheet*. Available at:
<https://shop.elkome.com/en/mwdownloads/download/link/id/1567/>. (accessed 22-05--10).
- Farrar CR and Worden K (2007) An introduction to structural health monitoring. *Philosophical Transactions of the Royal Society A: Mathematical, Physical and Engineering Sciences* Volume 365(Issue 1851): p. 303-315. Available at:
<https://royalsocietypublishing.org/doi/abs/10.1098/rsta.2006.1928> (accessed 2022-05-01).
- Haynes BP, Nunnington N and Eccles T (2017) *Corporate Real Estate Asset Management*. Routledge.
- HBM (n.d.-a) *newLight FS62 Optical Strain Sensor for Static and Dynamic Strain Measurements*. Available at: https://www.hbm.com/en/8120/newlight-fs62-optical-strain-sensor/?product_type_no=FS62%20Optical%20Strain%20Sensor. (accessed 2022-05-20).
- HBM (n.d.-b) *QuantumX: The Universal and Distributable Data Acquisition System*. Available at: https://www.hbm.com/en/2128/quantumx-compact-universal-data-acquisition-system/?product_type_no=QuantumX%20Data%20Acquisition%20System.
- HBM (n.d.-c) *What is a Fiber Bragg Grating?* Available at:
<https://www.hbm.com/en/4596/what-is-a-fiber-bragg-grating/>. (accessed 2022-05-20).

- Honfi D (2014) Serviceability floor loads. *Structural Safety* Volume 50: 27-38. Available at: <https://www.sciencedirect.com/science/article/pii/S0167473014000228>. (accessed 22-05-25).
- Isaksson T and Mårtensson A (2017) *Bygghkonstruktion - Regel och formelsamling*. Lund: Studentlitteratur AB.
- Isaksson T, Mårtensson A and Thelandersson S (2011) *Bygghkonstruktion*. Lund: Studentlitteratur AB.
- JCSS JCoSS (2001) JCSS PROBABILISTIC MODEL CODE - PART 2: LOAD MODELS. Available at: https://www.jcss-lc.org/publications/jcsspmc/live_load.pdf.
- Misra P, Mohini SK and Mishra SK (2014) The Design and Implementation of an ANN-based Non-linearity Compensator of LVDT Sensor. Available at: <http://arxiv.org/abs/1407.0506> (accessed 2022-02-16).
- Mitschke F (2016) *Fiber Optics Physics and Technology*. Berlin, Heidelberg SpringerLink (Online service) Available at: <https://search.ebscohost.com/login.aspx?direct=true&AuthType=ip,uid&db=cat07147a&AN=lub.5834468&site=eds-live&scope=site>
- Opkon (n.d.) *Model SLPS datasheet*. Available at: <https://www.opkon.com.tr/Content/product/pdf/pdf-9253c93f.pdf>.
- Pianigiani G (2020) *Poor Maintenance and Construction Flaws Are Cited in Italy Bridge Collapse*. Available at: <https://www.nytimes.com/2020/12/22/world/europe/genoa-bridge-collapse.html>. (accessed 2022-04-20).
- Polytec (n.d.-a) *Laser Doppler vibrometry*. Available at: <https://www.polytec.com/eu/vibrometry/technology/laser-doppler-vibrometry>. (accessed 2022-02-22).
- Polytec (n.d.-b) *RLV-5500 Rotational Laser Vibrometer*. Available at: <https://www.polytec.com/int/vibrometry/products/special-application-vibrometers/rlv-5500-rotational-laser-vibrometer?lhash=671a120474a5f439f754>. (accessed 22-05-20).
- Porteous J and Kermani A (2007) *Structural timber design to Eurocode 5*. Blackwell Publishing
- Sahota JK, Gupta N and Dhawan D (2020) Fiber Bragg grating sensors for monitoring of physical parameters: a comprehensive review. *OPTICAL ENGINEERING* Vol. 59(No.6). Available at: <https://www.spiedigitallibrary.org/journals/optical-engineering/volume-59/issue-06/060901/Fiber-Bragg-grating-sensors-for-monitoring->

[of-physical-parameters/10.1117/1.OE.59.6.060901.full?SSO=1&tab=ArticleLink](#).
(accessed 2022-02-10).

Sentler L (1974) Report 56: A Live Load Survey in Office Buildings and Hotels. Reportno. 56, Lund, Sweden: Lund Institute of Technology.

Sentler L (1975) Report 60: A Stochastic Model for Live Loads on Floors in Buildings. Reportno. 60, Lund, Sweden: Lund Institute of Technology.

Shmulsky R and Jones PD (2019) *Forest Products and Wood Science - An Introduction*.

SIS, Swedish Standards Institute, (1990) Eurocode - Basics of structural design. Epub ahead of print 1.

SIS, Swedish Standards Institute, (1991) Eurocode 1: Actions on structures - Part 1-1: General actions - Densities, self-weight, imposed loads for buildings.

SIS, Swedish Standards Institute, (1995) Eurocode 5: Design of timber structures.

Stefanescu DM (2011) *Handbook of Force Transducers - Principles and Components*. Berlin Heidelberg: Springer. Available at: http://xn--webducation-dbb.com/wp-content/uploads/2020/02/Dan-Mihai-Stefanescu-auth.-Handbook-of-Force-Transducers_-Principles-and-Components-Springer-Verlag-Berlin-Heidelberg-2011.pdf

Still GK (2019) *Static crowd density (general)*. Available at: <https://www.gkstill.com/Support/crowd-density/CrowdDensity-1.html>. (accessed 2022-05-06).

Storaenso (2017) *CLT by Stora Enso - Technical brochure*. Available at: <https://www.storaenso.com/-/media/documents/download-center/documents/product-brochures/wood-products/clt-by-stora-enso-technical-brochure-en.pdf>

Swedish Wood (2019) *The CLT Handbook*.

Swedish Work Environment Authority (2021) *Lokalernas storlek beror på verksamheten*. Available at: <https://www.av.se/inomhusmiljo/lokaler-och-arbetsutrymme/lokalernas-storlek/>. (accessed 2022-05-06).

Tokyo Measuring Instruments Lab (n.d.-a) *Low Elastic Strain Gauge Wood, Gypsum Use*. Available at: https://tml.jp/e/product/strain_gauge/wood_gypsume.html. (accessed 2022-02-02).

Tokyo Measuring Instruments Lab (n.d.-b) *Polyester Strain Gauges Pseries*. Available at: https://tml.jp/eng/documents/strain_gauge/Pseries.pdf.

Variohm (n.d.-a) *Load Cell - AL6N Series*. Available at: https://www.variohm.com/contentfiles/datasheets/AL6N_Load_Cell_1810_C.pdf. (accessed 22-05-19).

Variohm (n.d.-b) *Load Cell Accuracy*. Available at: <https://www.variohm.com/news-media/technical-blog-archive/load-cell-accuracy>. (accessed 22-05-25).

Variohm (n.d.-c) *What is a Linear Potentiometer?* Available at: <https://www.variohm.com/news-media/technical-blog-archive/what-is-a-linear-potentiometer-#:~:text=A%20linear%20potentiometer%20is%20a,internal%20slider%20or%20wipe r%20carrier>. (accessed 2022-05-1).

WorldGBC WGBC (2019) *New report: the building and construction sector can reach net zero carbon emissions by 2050*. Available at: <https://www.worldgbc.org/news-media/WorldGBC-embodied-carbon-report-published>. (accessed 2022-03-10).

Appendix A

Figure A.1 shows all the strain gauges attached to the underside of the slab.

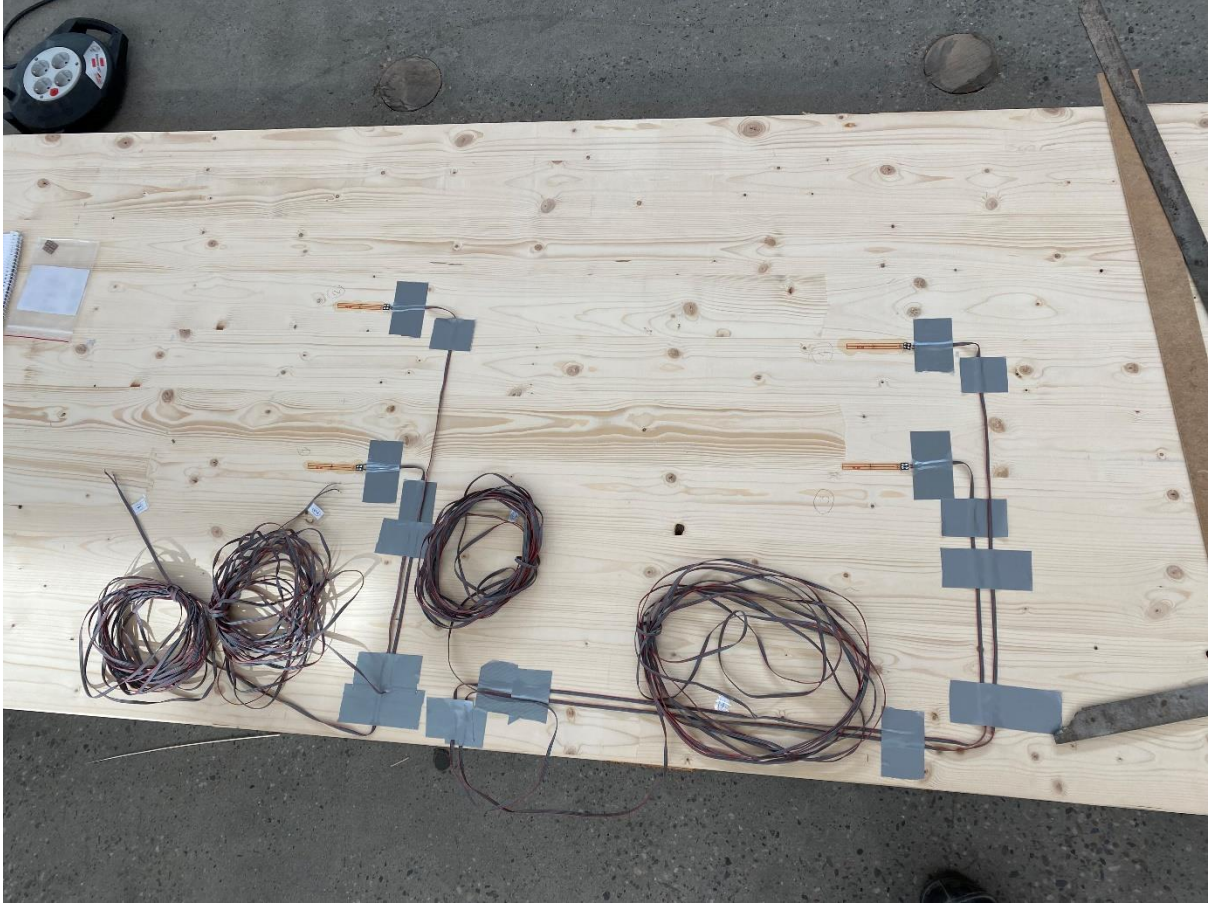


Figure A.9.1: All strain gauges attached to the underside of the slab

Appendix B

Figure B.1 depicts the test set up for load situations 1-7.

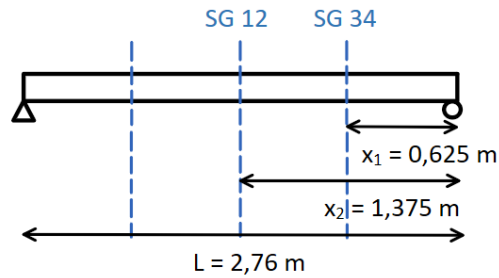


Figure B.1: Figure of the load set up for test 2, where two steel beams were placed on the slab depicting furniture such as chairs

Figure B.2 depicts the test set up for load situation 8 and 9.

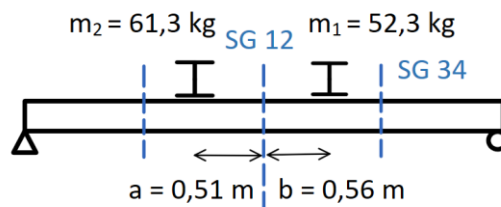


Figure B.2: Figure of the set up for load situation 8 and 9, where two steel beams were placed on the slab depicting furniture such as chairs

Figure B.3 depicts the test set up for load situation 10 shown in a side view in a) and from above in b).

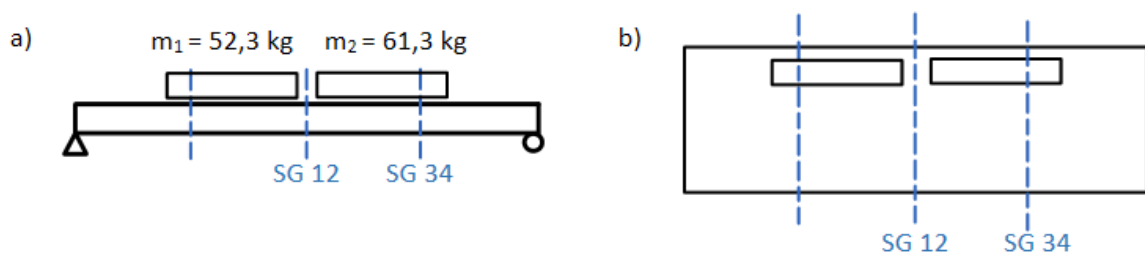


Figure B.3: A figure of the test set up for load situation 10. Two steel beams were placed on the slab in the load bearing direction to replicate the load of bookshelves in a real situation.

Figure B.4 shows the load situations in test 3.

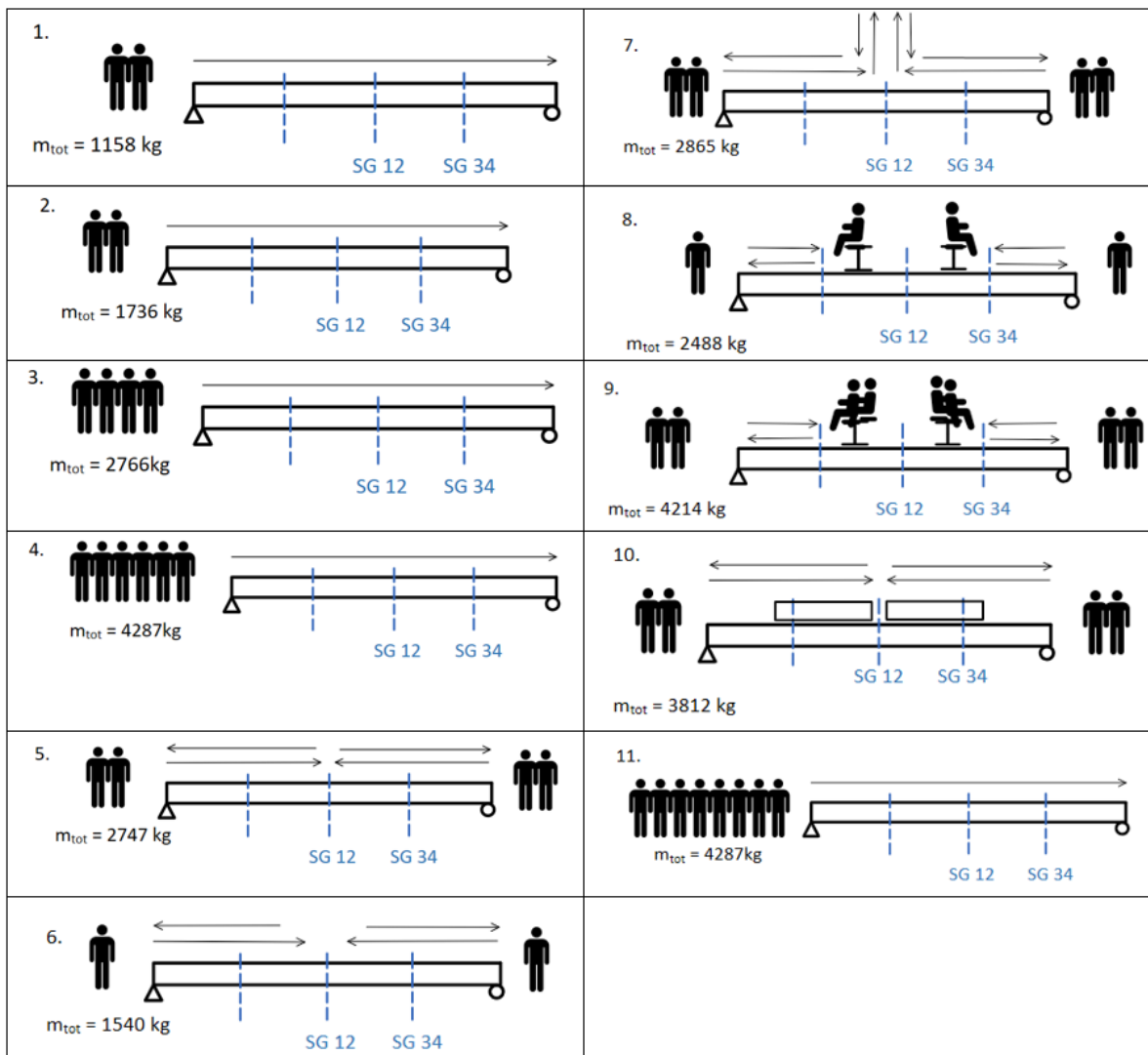


Figure B.4: The load situations in test 3.

Appendix C

The calculated bending stiffness for each measurement system and each load situation, for test 1, is shown in table 10. These values were used for the calculation of the average bending stiffness shown in table C.1.

Table C.1: Calculated bending stiffness.

Load situation	Bending stiffness (Nm) calculated from the respective measurement systems below:					
	Def 1	Def2	SG 1	SG 2	SG 3	SG 4
1	6,28E+05	6,51E+05	7,82E+05	7,59E+05	7,22E+05	7,31E+05
2	6,50E+05	6,54E+05	7,83E+05	7,61E+05	7,18E+05	7,22E+05
3	6,57E+05	6,52E+05	7,80E+05	7,59E+05	7,12E+05	7,13E+05

The measurement results from test 1 are shown in table C.2.

Table C.2: Measurement results from test 1.

Load situation	Time (s)	Load (kN)	Def piston (mm)	Def 1 (mm)	Def 2 (mm)	SG 1 - midpoint ($\mu\text{m}/\text{m}$)	SG 2 ($\mu\text{m}/\text{m}$)	SG 3 - quarter point ($\mu\text{m}/\text{m}$)	SG 4 ($\mu\text{m}/\text{m}$)
1	100	12,14	16,27	8,47	8,17	482,07	496,76	236,53	233,53
2	360	19,94	21,72	13,44	13,36	791,02	813,88	390,72	388,46
3	850	29,94	28,40	19,96	20,12	1190,95	1224,21	591,07	590,40

The central point loads for test 1 are shown in table C.3 below.

Table C.3: The central point loads calculated for test 1.

Load situation	Load (kN)	Bending stiffness used:	Load (N) calculated from the respective measurement systems below:						
			Def piston	Def 1	Def 2	SG 1	SG 2	SG 3	SG 4
1	12,14	theoretical	19,92	10,37	10,00	8,33	8,58	8,17	8,07
		calibrated		12,54	12,10	11,97	12,33	12,10	11,95
2	19,94	theoretical	26,59	16,45	16,36	13,66	14,06	13,50	13,42
		calibrated		19,90	19,78	19,63	20,20	20,00	19,88
3	29,94	theoretical	34,77	24,44	24,64	20,57	21,14	20,42	20,39
		calibrated		29,55	29,79	29,56	30,39	30,25	30,21

Appendix D

Measurement results from the sensors during test 2 are presented in table D.1.

Table D.1: Measurement results from test 2

load situation	Time (s)	Load (N)	Def 1 (mm)	Def 2 (mm)	SG 1 - midpoint ($\mu\text{m}/\text{m}$)	SG 2 ($\mu\text{m}/\text{m}$)	SG 3 - quarter point ($\mu\text{m}/\text{m}$)	SG 4 ($\mu\text{m}/\text{m}$)
1	175	533	0,23	0,42	10,33	12,30	23,74	17,34
2	250	1134,04	0,41	0,69	18,17	20,66	43,37	32,95
3	300	1134,04	0,64	0,82	24,72	27,46	39,09	30,70
4	350	1134,04	0,85	0,91	30,70	34,05	32,10	27,49
5	575	601,35	0,33	0,43	10,05	12,13	6,67	4,84
6	660	1134,04	0,61	0,65	17,93	20,65	11,04	9,20
7	725	1134,04	0,81	0,69	24,71	26,54	14,76	12,01
8	800	1134,04	1,04	0,70	32,04	33,58	18,92	15,45
9	900	1134,04	0,87	0,85	31,85	33,53	25,98	21,33

The results in table D.1 were used to calculate the following noncentral loads presented in table D.2.

Table D.2: The calculated non-central loads

Load situation	Calculated with bending stiffness:	Load (N)	Load (N) calculated from the respective measurement systems below:					
			Def 1	Def2	SG 1	SG 2	SG 3	SG 4
1	Theoretical	533	504	912	446	531	665	486
	Calibrated		610	1103	641	763	892	652
2	Theoretical	1134	885	1488	785	892	1215	923
	Calibrated		1070	1800	1128	1282	1630	1238
4	Theoretical	1134	1147	1233	715	793	1048	897
	Calibrated		1407	1512	1053	1168	1285	1100
5	Theoretical	602	720	931	434	524	638	463
	Calibrated		870	1126	624	753	856	621
6	Theoretical	1134	1314	1406	774	892	1057	880
	Calibrated		1589	1700	1112	1281	1418	1181
8	Theoretical	1134	1409	950	746	782	976	797
	Calibrated		1704	1149	1080	1132	1310	1070

The uniformly distributed load and the point load were also calculated and are shown in table D.3 below.

Table D.3: The central point load (Q_k) and the uniformly distributed load (q_k) calculated from measurement results for test 2.

load situation	Load (N)	load type information	Load calculated from the respective measurement systems below:					
			Def 1	Def2	SG 1	SG 2	SG 3	SG 4
1	533	q_k (N/ m ²)	200	362	186	221	569	416
		Q_k (N)	345	624	513	611	1215	887
2	1134	q_k (N/ m ²)	351	591	327	372	1040	790
		Q_k (N)	606	1019	902	1026	2220	1686
3	1134	q_k (N/ m ²)	547	703	445	494	937	736
		Q_k (N)	944	1212	1227	1363	2000	1571
4	1134	q_k (N/ m ²)	729	783	552	612	769	659
		Q_k (N)	1258	1351	1524	1690	1643	1407
5	601	q_k (N/ m ²)	286	370	181	218	160	116
		Q_k (N)	493	637	499	602	341	247
6	1134	q_k (N/ m ²)	521	558	322	371	265	220
		Q_k (N)	900	963	890	1025	565	471
7	1134	q_k (N/ m ²)	692	589	444	477	354	288
		Q_k (N)	1194	1017	1227	1318	755	614
8	1134	q_k (N/ m ²)	896	604	576	604	453	370
		Q_k (N)	1545	1042	1591	1667	968	791
9	1134	q_k (N/ m ²)	747	730	573	603	623	511
		Q_k (N)	1288	1259	1581	1664	1329	1092

Appendix E

Measurement results from the measurement systems during test 3 are shown in table E.1.

Table E.1: Measurement results for test 3

Load situation	time (s)	Load (N)	Def 1 (mm)	Def 2 (mm)	SG 1 ($\mu\text{m}/\text{m}$)	SG 2 ($\mu\text{m}/\text{m}$)	SG 3 ($\mu\text{m}/\text{m}$)	SG 4 ($\mu\text{m}/\text{m}$)
1	16,5	1158	0,56	0,61	17,17	17,19	22,44	15,04
2	26,5	1736	0,56	0,76	15,78	16,86	27,15	21,52
3	44,5	2766	1,63	2,38	78,03	73,71	58,22	45,56
4	75,5	4287	3,00	3,12	115,62	118,93	94,49	77,83
5	105,5	2747	1,90	2,26	81,16	79,13	57,16	43,98
6	150,5	1540	1,09	1,63	56,47	55,07	32,74	17,84
7	176,5	2865	2,09	2,19	78,29	81,18	55,47	39,44
8	290,5	2487	1,45	1,84	52,04	51,65	50,18	29,78
9	315,5	4214	2,33	3,15	93,08	89,18	86,51	60,08
10	385,0	3812	2,17	3,09	101,90	98,08	75,63	47,04
11	441,0	6892	3,82	3,92	145,02	143,98	118,30	95,33

The calculated load results for test 3 are presented in table E.2.

Table E.2: The central point load (Q_k) and the uniformly distributed load (q_k) calculated from measurement results for test 3.

Load situation	Real point load not central (N)	Load (N) calculated from the respective measurement systems below:						
		Load type	Def 1	Def2	SG 1	SG 2	SG 3	SG 4
1	1158	q_k (N/ m ²)	483	526	309	309	538	360
		Q_k (N)	833	907	796	797	1148	769
2	1736	q_k (N/ m ²)	484	653	284	303	651	516
		Q_k (N)	836	1126	731	781	1389	1101
3	2766	q_k (N/ m ²)	1400	2046	1403	1326	1396	1092
		Q_k (N)	2415	3529	3617	3417	2979	2331
4	4287	q_k (N/ m ²)	2575	2679	2080	2139	2265	1866
		Q_k (N)	4441	4621	5359	5513	4835	3983
5	2747	q_k (N/ m ²)	1631	1940	1460	1423	1370	1054
		Q_k (N)	2813	3347	3762	3668	2925	2251
6	1540	q_k (N/ m ²)	938	1395	1016	990	785	428
		Q_k (N)	1618	2406	2618	2553	1675	913
7	2865	q_k (N/ m ²)	1792	1882	1408	1460	1330	945
		Q_k (N)	3092	3246	3629	3763	2839	2018
8	2488	q_k (N/ m ²)	1242	1577	936	929	1203	714
		Q_k (N)	2142	2720	2412	2394	2568	1524
9	4214	q_k (N/ m ²)	2002	2700	1674	1604	2074	1440
		Q_k (N)	3453	4658	4315	4134	4427	3075
10	3812	q_k (N/ m ²)	1866	2654	1833	1764	1813	1127
		Q_k (N)	3220	4578	4723	4546	3870	2407
11	6892	q_k (N/ m ²)	3278	3363	2608	2590	2836	2285
		Q_k (N)	5655	5801	6722	6674	6054	4878

Appendix F

Measurement results from the measurement systems during test 4 are presented in table F.1.

Table F.1: Measurement results from test 4

Load situation	Time (s)	Def 1 (mm)	Def 2 (mm)	SG 1 midpoint ($\mu\text{m}/\text{m}$)	SG 2 ($\mu\text{m}/\text{m}$)	SG 4 quarter point ($\mu\text{m}/\text{m}$)
1 a)	40,5	0,34	0,24	8,85	9,53	7,06
1 b)	80	0,57	0,74	19,41	19,95	22,14
1 c)	110	0,24	0,51	10,57	10,57	15,50
2	125	0,38	0,57	20,15	20,09	12,44
3 a)	148	0,40	0,26	11,27	12,30	5,64
3 b)	167	0,68	0,51	20,54	21,90	10,72
3 c)	230	0,43	0,25	11,54	13,05	5,35
4	265	0,39	0,59	19,76	20,63	6,71

The results in table F.1 were used to calculate the loads in table F.2.

Table F.2: The central point load (Q_k) and the uniformly distributed load (q_k) and the average load calculated from the measurement results.

Loads calculated from the respective measurement systems below:							
Load situation	Load type	Def 1	Def 2	SG 1 - midpoint	SG 2	SG 4 - quarter point	Average load
1 a)	q_k (N/ m ²)	288	208	159	171	169	199
	Q_k (N)	496	359	440	473	361	426
1 b)	q_k (N/ m ²)	493	637	349	359	531	474
	Q_k (N)	850	1100	963	990	1133	1007
1 c)	q_k (N/ m ²)	208	441	190	190	372	280
	Q_k (N)	359	761	525	525	793	593
2	q_k (N/ m ²)	330	490	362	361	298	368
	Q_k (N)	569	845	1000	997	637	810
3 a)	q_k (N/ m ²)	342	225	203	221	135	225
	Q_k (N)	590	387	560	611	288	487
3 b)	q_k (N/ m ²)	582	436	370	394	257	408
	Q_k (N)	1004	752	1020	1087	549	882
3 c)	q_k (N/ m ²)	370	214	208	235	128	231
	Q_k (N)	639	370	573	648	274	501
4	q_k (N/ m ²)	332	505	355	371	161	345
	Q_k (N)	572	872	981	1024	343	759